The effect of measurement errors on the performance of the homogenously weighted moving average X^- monitoring scheme

Maonatlala Thanwane, Jean-Claude Malela-Majika, Philippe Castagliola, Sandile Charles Shongwe

The effect of measurement errors on the performance of the homogenously weighted moving average $\bar{X}$ monitoring scheme

Maonatlala Thanwane[1], Jean-Claude Malela-Majika[1], Philippe Castagliola[2], Sandile Charles Shongwe[1]

[1] Department of Statistics, College of Science, Engineering and Technology, University of South Africa, PO Box 392 UNISA 0003, Pretoria, South Africa

[2] Département Qualité Logistique Industrielle et Organisation, Université de Nantes & LS2N UMR CNRS 6004, Nantes, France.

Abstract

Monitoring schemes are typically designed under the assumption of perfect measurements. However, in real-life applications, data tend to be subjected to measurement errors, i.e., a difference between the real quantities and the measured ones mostly exist even with highly sophisticated advanced measuring instruments. Thus, in this paper, the negative effect of measurement errors on the performance of the homogenously weighted moving average (HWMA) scheme is studied using the linear covariate error model for constant and linearly increasing variance. Monte Carlo simulations are used to evaluate the performance of the proposed HWMA scheme in terms of the run-length characteristics. It is observed that as the smoothing parameter increases, measurement errors have a higher negative effect on the performance of the HWMA $\bar{X}$ scheme. More importantly, it is shown that the negative effect of measurement errors is reduced by using multiple measurements and / or by increasing the slope coefficient of the covariate error model. Moreover, the performance of the HWMA $\bar{X}$ scheme is compared with the corresponding exponentially weighted moving average (EWMA) and Cumulative Sum (CUSUM) $\bar{X}$ schemes. An illustrative example is provided to help in implementing this monitoring scheme in a real-life situation.

Keywords: Homogenously Weighted Moving Average scheme; Linear covariate error model; Linearly increasing variance; Measurement error; Multiple measurements.

Introduction

In statistical process monitoring (SPM), control charts are used to identify the causes of variation in the process. Two sources of variation can be distinguished in SPM, namely the common (or chance) causes and the assignable (or special) causes of variation. Common causes cannot be avoided, while assignable causes of variation need to be reduced as much as possible. When the process runs in the presence of common causes only, the process is considered to be in-control (IC). Otherwise, the process is said to be out-of-control (OOC). When practitioners are interested in monitoring small-to-moderate shifts in the process parameters, popular memory-type monitoring schemes such as the Cumulative Sum (CUSUM) and exponentially weighted moving average (EWMA) schemes are mostly recommended; see for example, Roberts (1959), Page (1961) and Montgomery (2013). Many authors devoted their valuable time in improving the sensitivity of the CUSUM and EWMA schemes using various techniques. These enhanced schemes include the double CUSUM (DCUSUM), hybrid EWMA (HEWMA), double EWMA (DEWMA), Synthetic CUSUM, Synthetic EWMA, etc. For more details on the enhancement of memory-type schemes, readers are referred to Waldmann (1996), Capizzi and Masarotto (2010), Abbas et al. (2013), Haq et al. (2013), Ali and Haq (2017), Adeoti (2020), Malela-Majika (2020); just to cite a few. For other alternative approaches of control charts, such as the use of divergence functions (e.g. parametric and nonparametric Kullback-Leibler Divergence), see for instance Bakdi and Kouadri (2018), Bakdi et al. (2019) and Bounoua et al. (2020).

More recently, Abbas (2018) developed a new memory-type scheme that allocates a specific weight to the current sample and the remaining weight is distributed equally among the previous samples; this scheme

is known as homogeneously weighted moving average (HWMA) monitoring scheme. The HWMA scheme is in its nature a memory-type scheme used to effectively monitor small-to-moderate shifts (see for example the following articles on the HWMA-type monitoring schemes: Abbas (2018), Adegoke et al. (2019a, b), Raza et al. (2020), Abid et al. (2020), Abbas et al. (2020) and Adeoti and Koleoso (2020)). To provide an efficient and unbiased estimate of the process mean, Adegoke et al. (2019a) developed a HWMA scheme to monitor the process mean that uses the auxiliary variable in the form of a bivariate regression estimator. Next, Adegoke et al. (2019b) proposed a multivariate HWMA scheme for monitoring the process mean vector when the underlying distribution parameters are known; more recently though, Abbas et al. (2020) studied the same scheme when the underlying distribution parameters are assumed unknown and they compared its performance against numerous well-known multivariate schemes. Raza et al. (2020) proposed a distribution-free HWMA scheme based on the sign and signed-rank statistics to monitor skewed and symmetric distributions observations. More recently, Abid et al. (2020) proposed the double HWMA scheme for monitoring small shifts in the process mean and they also investigated the effect of non-normality and parameter estimation on the performance of the double HWMA scheme. Finally, Adeoti and Koleoso (2020) proposed a hybrid HWMA schemes for monitoring the process mean and they also investigated the effect of non-normality. Note that the double (hybrid) design of the HWMA scheme entails applying the same (different) smoothing parameter twice, respectively. The key difference between the HWMA scheme proposed in this paper and the abovementioned HWMA schemes is that it is not assumed that the observations have perfect or exact measurements. That is, in this paper, the assumption given in the review paper by Maleki et al. (2017) is followed: '… exact measurements in real-life applications are a rare phenomenon, even with highly sophisticated advanced measuring instruments; hence, measurement errors tend to exist in any manufacturing and service environment'. Therefore, this paper contributes to the SPM literature by

introducing an HWMA scheme that accounts for measurement errors in the process being monitored for a univariate process mean.

A detailed early account of 60 articles on monitoring schemes with measurements errors are documented in Maleki et al. (2017). To discuss a few, Linna and Woodall (2001) studied the effect of measurement errors on Shewhart monitoring scheme and they reported that under measurement errors a monitoring scheme is exposed to lose power in detecting parameters shifts. Next, Maravelakis et al. (2004) and Maravelakis (2012) investigated the effect of measurement errors on the EWMA and CUSUM schemes, respectively; with the effect of a two-component measurement error on the EWMA scheme investigated in Abbasi (2016). For some recent discussions on measurement errors published after the review paper of Maleki et al. (2017), see for instance: Yeong et al. (2017), Cheng and Wang (2018), Salmasnia et al. (2018), Tang et al. (2019), Riaz et al. (2019), Tran et al. (2019a, b, c, 2020), Nguyen et al. (2019), Zaidi et al. (2019, 2020), Sabahno et al. (2019, 2020), Shongwe et al. (2020a, b, c), Asif et al. (2020), Noor-ul-Amin et al. (2020).

A number of methods used as remedial approaches are outlined in the review article on measurement errors by Maleki et al. (2017) – for other remedial sampling strategies, see for instance the book by Aslam and Ali (2019). The most used methodology to reduce measurement inaccuracy is by taking multiple measurements of each item, which was first proposed by Linna and Woodall (2001). The multiple measurements strategy reduces the effect of measurement errors on the performance of monitoring schemes. That is, taking at least two measurements for each sampled unit effectively reduces the effect of the measurement errors. The level of precision improves by taking and averaging several measurements. Although it is preferable to maintain a larger number of multiple measurements for better results, one needs to be mindful of additional implications such as costs and time to collect these observations. This is so because, without measurement error, multiple measurements will become redundant in the monitoring scheme methodology by only adding costs for measuring extra and useless observations.

Therefore, in this paper, the performance of the HWMA scheme for monitoring the process mean (denoted as HWMA $\bar{X}$ scheme) is investigated under the effect of measurement errors. The measurement errors are modelled by a linear covariate error model. The negative effect of the measurement errors on the proposed HWMA $\bar{X}$ scheme is reduced by using a multiple measurements strategy and / or by increasing the slope coefficient of the linear covariate error model.

The rest of this paper is organised as follows: in the second section, the basic properties of the HWMA $\bar{X}$ scheme without measurement errors are provided. Third section provides properties of the HWMA $\bar{X}$ scheme with measurement errors using a covariate error model with a constant and a linearly increasing variance. The performance of the HWMA $\bar{X}$ scheme with a constant and a linearly increasing variance is studied in terms of the average run-length (*ARL*), standard deviation of the run-length (*SDRL*) and expected *ARL* (*EARL*) values in the fourth section. Moreover, in the fourth section, the HWMA $\bar{X}$ scheme is compared with the corresponding CUSUM and EWMA $\bar{X}$ schemes. Two illustrative examples using real-life data are given in the fifth section. Some concluding remarks are presented in the sixth section and the simulation algorithm is provided in the Appendix.

Design of the HWMA $\bar{X}$ scheme

Let X_{ij} $\{i = 1, 2, \ldots,$ and $j = 1, 2, \ldots, n\}$ be a set of samples of independent normal random variables, i.e. X_{ij} follows a $N(\mu_0 + \delta\sigma_0, \sigma_0)$, where μ_0 is the in-control mean value, σ_0 is the in-control standard deviation and δ is the magnitude of the shift in standard deviation units. When $\delta = 0$, the process is considered to be IC, which implies X_{ij} follows a $N(\mu_0, \sigma_0)$. However, when $\delta \neq 0$ the process is OOC. Let $\bar{X}_i$ $(= \sum_{j=1}^{n} X_{ij}/n)$ be the sample mean of the i^{th}sample. The plotting statistic of the HWMA $\bar{X}$ scheme (denoted as H_i) is defined by

$$H_i = \lambda\bar{X}_i + (1 - \lambda)\,\bar{\bar{X}}_{i-1}, \tag{1}$$

with

$$\bar{\bar{X}}_{i-1} = \frac{\sum_{v=1}^{i-1} \bar{X}_v}{i-1},$$

where λ ($0 < \lambda \leq 1$) is the smoothing constant and $\bar{\bar{X}}_{i-1}$ is the mean of the previous $i-1$ sample means. The initial value of $\bar{\bar{X}}_{i-1}$ (i.e. $\bar{\bar{X}}_0$) is typically set to be equal to the target mean μ_0.

Abbas (2018) showed that Equation (1) can also be written as

$$H_i = \lambda \bar{X}_i + \left[\left(\frac{1-\lambda}{i-1}\right)\bar{X}_{i-1} + \left(\frac{1-\lambda}{i-1}\right)\bar{X}_{i-2} + \cdots + \left(\frac{1-\lambda}{i-1}\right)\bar{X}_2 + \left(\frac{1-\lambda}{i-1}\right)\bar{X}_1\right]. \quad (2)$$

From Equation (2), it can be seen that the HWMA $\bar{X}$ statistic assigns weight λ to the current sample and a weight $(1-\lambda)$ is equally distributed to the previous samples. It can be shown that the mean and variance of the plotting statistic in Equation (1) or (2) is given by

$$E(H_i) = \mu_0$$

and (3)

$$Var(H_i) = \sigma_{H_i}^2 = \begin{cases} \frac{\lambda^2\sigma_0^2}{n}, & if\ i = 1 \\ \frac{\lambda^2\sigma_0^2}{n} + \frac{(1-\lambda)^2\sigma_0^2}{n(i-1)}, & if\ i > 1 \end{cases}$$

respectively. Therefore, the time-varying lower and upper control limits (i.e. LCL and UCL) of the HWMA $\bar{X}$ monitoring scheme are defined by

$$LCL_i = \begin{cases} \mu_0 - L\sqrt{\frac{\lambda^2\sigma_0^2}{n}}, & i = 1 \\ \mu_0 - L\sqrt{\frac{\lambda^2\sigma_0^2}{n} + \frac{(1-\lambda)^2\sigma_0^2}{n(i-1)}}, & i > 1 \end{cases}$$

and (4)

$$UCL_i = \begin{cases} \mu_0 + L\sqrt{\dfrac{\lambda^2\sigma_0^2}{n}}, & i = 1 \\ \mu_0 + L\sqrt{\dfrac{\lambda^2\sigma_0^2}{n} + \dfrac{(1-\lambda)^2\sigma_0^2}{n(i-1)}}, & i > 1 \end{cases}$$

respectively; where L is the control limits constant that is set to have a pre-specified false alarm rate or in-control ARL (ARL_0). Thus, the HWMA $\bar{X}$ scheme gives a signal if the plotting statistic in Equation (1) plots beyond the control limits defined in Equation (4); that is, if $H_i \geq UCL_i$ or $H_i \leq LCL_i$. In case the process has been running for a long time (i.e. $i \to \infty$), the term $\frac{(1-\lambda)^2}{i-1} \to 0$. Therefore, the control limits in Equation (4) reduce to the following asymptotic ones

$$LCL = \mu_0 - L\sqrt{\frac{\lambda^2\sigma_0^2}{n}},$$

and (5)

$$UCL = \mu_0 + L\sqrt{\frac{\lambda^2\sigma_0^2}{n}},$$

and, in this case, the process is OOC if $H_i \geq UCL$ or $H_i \leq LCL$.

The HWMA scheme with measurement errors

Covariate error model with a constant variance

Assume that the true value of the quality characteristic $X_{i,j}$ defined in the second section is only observed through a value $\{X^*_{i,j,k}: i = 1,2,\ldots;\ j = 1,2,\ldots, n;\ k = 1,\ldots, r\}$ described by the expression $X^*_{i,j,k} = A + BX_{i,j} + \varepsilon_{i,j,k}$, where A and B are two constants depending on the measurement system location error (A and B are also known as the intercept and slope coefficients of the covariate error model, respectively). Also, r denotes the number of measurements taken in each sampled subgroup unit and $\varepsilon_{i,j,k} \sim N(0, \sigma_m^2)$ is a random error due to the measurement error that is distributed independently of $X_{i,j}$; where σ_m^2 is the

variance of the measurement system. Based on the discussion in Linna and Woodall (2001) and Maravelakis et al. (2004), it is apparent that $X^*_{i,j,k} \sim N(A + B\mu_0, B^2\sigma_0^2 + \sigma_M^2)$. Assuming that n observations from the sequence $X^*_{i,j,k}$ at each sampling point have been collected, the mean

$$\bar{X}^*_i = \frac{1}{nr}\sum_{j=1}^{n}\sum_{k=1}^{r} X^*_{i,j,k} = \frac{1}{nr}\sum_{j=1}^{n}\sum_{k=1}^{r}(A + BX_{i,j} + \varepsilon_{i,j,k}) = A + B\frac{1}{n}\sum_{j=1}^{n} X_{i,j} + \frac{1}{nr}\sum_{j=1}^{n}\sum_{k=1}^{r}\varepsilon_{i,j,k}$$

need to be calculated. Thus, the plotting statistic of the HWMA $\bar{X}^*$ scheme is defined by

$$H^*_i = \lambda\bar{X}^*_i + (1-\lambda)\,\bar{\bar{X}}^*_{i-1}, \tag{6}$$

where $\bar{\bar{X}}^*_{i-1}$ is the mean of the previous $i-1$ sample means and similarly as in Equation (2), Equation (6) can be written as

$$H^*_i = \lambda\bar{X}^*_i + \left[\left(\frac{1-\lambda}{i-1}\right)\bar{X}^*_{i-1} + \left(\frac{1-\lambda}{i-1}\right)\bar{X}^*_{i-2} + \cdots + \left(\frac{1-\lambda}{i-1}\right)\bar{X}^*_2 + \left(\frac{1-\lambda}{i-1}\right)\bar{X}^*_1\right].$$

The initial value of $\bar{\bar{X}}^*_{i-1}$ (i.e. $\bar{\bar{X}}^*_0$) is typically set to be equal to the target mean μ_0. Thus, the expected value and variance of the plotting statistic H^*_i defined in Equation (6) are

$$E(H^*_i) = A + B\mu_0$$

and (7)

$$Var(H^*_i) = \sigma^2_{H^*_i} = \begin{cases} \lambda^2\dfrac{rB^2\sigma_0^2 + \sigma_m^2}{nr}, & if\ i = 1 \\ \left[\lambda^2 + \dfrac{(1-\lambda)^2}{i-1}\right]\dfrac{rB^2\sigma_0^2 + \sigma_m^2}{nr}, & if\ i > 1. \end{cases}$$

Let $\gamma = \frac{\sigma_m}{\sigma_0}$ represents the standardized ratio of the measurement system variability to the process variability. When $\bar{X}_i$ is from a perfect measurement system, then σ_m = 0, so that $\gamma = 0$; otherwise, $\gamma > 0$. The time-varying control limits of the HWMA $\bar{X}^*$ scheme with r-measurements are defined by:

$$LCL_i = \begin{cases} A + B\mu_0 - L^* \sqrt{\dfrac{\lambda^2\sigma_0^2}{n}\left(\dfrac{rB^2+\gamma^2}{r}\right)}, & i = 1 \\ A + B\mu_0 - L^* \sqrt{\left(\dfrac{\lambda^2\sigma_0^2}{n} + \dfrac{(1-\lambda)^2\sigma_0^2}{n(i-1)}\right)\left(\dfrac{rB^2+\gamma^2}{r}\right)}, & i > 1 \end{cases}$$

and (8)

$$UCL_i = \begin{cases} A + B\mu_0 + L^* \sqrt{\dfrac{\lambda^2\sigma_0^2}{n}\left(\dfrac{rB^2+\gamma^2}{r}\right)}, & i = 1 \\ A + B\mu_0 + L^* \sqrt{\left(\dfrac{\lambda^2\sigma_0^2}{n} + \dfrac{(1-\lambda)^2\sigma_0^2}{n(i-1)}\right)\left(\dfrac{rB^2+\gamma^2}{r}\right)}, & i > 1 \end{cases}$$

where L^* is control limit width parameter of the HWMA $\bar{X}^*$ scheme with r-measurements.

Since the term $\frac{(1-\lambda)^2}{i-1} \to 0$ when the process has been running for a while, the asymptotic control limits of the HWMA $\bar{X}^*$ scheme with r-measurements are defined by

$$LCL = A + B\mu_0 - L^* \sqrt{\frac{\lambda^2\sigma_0^2}{n}\left(\frac{rB^2+\gamma^2}{r}\right)}$$

and (9)

$$UCL = A + B\mu_0 + L^* \sqrt{\frac{\lambda^2\sigma_0^2}{n}\left(\frac{rB^2+\gamma^2}{r}\right)}.$$

The value of r is equal to 1 when a standard single measurement is used per sampling unit. However, as r increases, the variance in the measurement error component decreases. Hence, it is obvious that when the number of multiple components tends to infinity, the variance in the measurement component tends to zero. However, the number of sets of measurements needs to be determined such that the maximum reduction in the variance of the measurement system is reached and, at the same time, minimizes the cost of using multiple measurements. This is addressed in the fourth section.

Covariate error model with a linearly increasing variance

In some situations, the measurement error σ_m should no longer be considered as being a constant but it should be considered as an increasing function of the mean of the variable $X_{i,j}$, i.e. $\sigma_m^2 = C + D\mu_0$ and thus, $X_{i,j,k}^* \sim N(A + B\mu_0, B^2\sigma_0^2 + C + D\mu_0)$. Then the time-varying control limits of the HWMA $\bar{X}^*$ scheme with r-measurements are defined by:

$$LCL_i = \begin{cases} A + B\mu_0 - L^* \sqrt{\lambda^2 \left(\dfrac{rB^2\sigma_0^2 + C + D\mu_0}{nr} \right)}, & i = 1 \\ A + B\mu_0 - L^* \sqrt{\left(\lambda^2 + \dfrac{(1-\lambda)^2}{i-1} \right) \left(\dfrac{rB^2\sigma_0^2 + C + D\mu_0}{nr} \right)}, & i > 1 \end{cases}$$

and (10)

$$UCL_i = \begin{cases} A + B\mu_0 + L^* \sqrt{\lambda^2 \left(\dfrac{rB^2\sigma_0^2 + C + D\mu_0}{nr} \right)}, & i = 1 \\ A + B\mu_0 + L^* \sqrt{\left(\lambda^2 + \dfrac{(1-\lambda)^2}{i-1} \right) \left(\dfrac{rB^2\sigma_0^2 + C + D\mu_0}{nr} \right)}, & i > 1 \end{cases}$$

where C and D are constants. Next, the asymptotic control limits of the HWMA $\bar{X}^*$ scheme with r-measurements are defined by:

$$LCL = A + B\mu_0 - L^* \sqrt{\lambda^2 \left(\frac{rB^2\sigma_0^2 + C + D\mu_0}{nr} \right)}$$

and (11)

$$UCL = A + B\mu_0 + L^* \sqrt{\lambda^2 \left(\frac{rB^2\sigma_0^2 + C + D\mu_0}{nr} \right)},$$

To conserve space, in this paper, the focus is on the time-varying case.

Performance of the HWMA $\bar{X}^*$ scheme with measurement errors

One of the most popular measures used to evaluate the performance of a monitoring scheme is the ARL. The ARL is the mean of the run-length (RL) distribution representing the average number of rational subgroups plotted on a control chart before it gives a signal for the first time. This metric reveals the degree of the sensitivity of a monitoring scheme towards specific shifts. Depending on the type of monitoring scheme, the *ARL* metric can be computed using Markov chain, Monte Carlo simulation or integral or exact formulas. Among these techniques, Monte Carlo simulation is the most used because of its simplicity in computing the characteristics of the run-length distribution even for complicated and complex monitoring designs. In this paper, Monte Carlo simulation is used to compute the *ARL*, *SDRL* and *EARL* profiles of the HWMA $\bar{X}^*$ scheme in SAS® v9.4, see the Appendix for an outline of the simulation algorithm. Note that the *EARL* metric is used to investigate the performance of a scheme for a range of shifts. The *EARL* is mathematically defined by (see for example Umar et al. (2019), Shongwe et al. (2020a))

$$EARL = \frac{1}{\Delta}\sum_{\delta=\delta_{min}}^{\delta_{max}} ARL(\delta)\,, \tag{12}$$

where $\delta_{\min}$ and $\delta_{\max}$ are the lower and upper bound of the shift (δ) parameter, respectively, $ARL(\delta)$ is the *ARL* value for a specific shift δ and Δ represents the number of increments between $\delta_{\min}$ and $\delta_{\max}$.

Sensitivity analysis

In this section, the effect of measurement errors and multiple measurements on the performance of the HWMA $\bar{X}^*$ scheme is investigated in terms of the *ARL* and *SDRL* profiles for specific shifts and *EARL* profile for different ranges of shifts. Thus, the $EARL$ values denoted by $EARL_1$, $EARL_2$,$EARL_3$, $EARL_4$, $EARL_5$ and $EARL_6$ are used to investigate the performance of the HWMA $\bar{X}^*$ scheme for small ($0 < \delta \leq 1$), moderate ($1 < \delta \leq 2$), large ($2 < \delta \leq 3$), small-to-moderate ($0 < \delta \leq 2$), moderate-to-large ($1 <$

$\delta \leq 3$) and small-to-large ($0 < \delta \leq 3$) shifts, respectively. Tables 1 presents the *ARL* and *EARL* profiles of the HWMA $\bar{X}^*$ scheme when $\lambda \in \{0.1, 0.5, 0.9\}$, $\gamma \in \{0, 0.2, 0.5, 0.9\}$ and $r = 1$ on the first row (with $r = 4$ in parenthesis on the second row) for a nominal ARL_0 value of 500; while, Table 2 displays the corresponding *SDRL* profiles. Note that the manner in which the smoothing parameter (λ) is chosen depends on the size of the shifts that a practitioner prioritizes; see Abbas (2018). For instance, λ = 0.1 is recommended for a quick detection of small shifts, λ = 0.5 for moderate and large shifts and λ = 0.9 for a quick detection of very large shifts. Next, the level of measurements errors (γ) indicates the level of severity of the measurement error, where γ = 0 implies perfect measurements (i.e. no measurement error), γ = 0.2 indicates lower level of measurement error, γ = 0.5 indicates moderate level of measurement errors and γ = 0.9 indicates higher level of measurement error. From Tables 1 and 2 as well as Figures 1 and 2, the following is observed for any value of A and B=1:

- The design parameter L^* (shown at the bottom of Tables 1 and 2) increases as λ increases; which means, the larger the smoothing parameter, the wider are the control limits. Note that the control limits do not depend on the degree of measurement errors (i.e., γ value) nor on the number of measurements (i.e., r value).
- Measurement errors have a negative effect on the sensitivity of the HWMA $\bar{X}^*$ monitoring scheme, which means the higher the value of γ, the higher are the values of the ARL_1 profile. For instance, when $\lambda = 0.1$ and $r = 1$, for a small shift of size δ=0.25, if $\gamma = 0.5$ and 0.9, the HWMA $\bar{X}^*$ scheme is expected to give a signal on the 95th and 123rd subgroups, respectively.
- When γ is kept fixed, the HWMA $\bar{X}^*$ scheme is more sensitive to small values of λ for small and moderate shifts in the process mean. However, for large shifts, the sensitivity of the HWMA $\bar{X}^*$ scheme increases in the interval $0 < \lambda < 0.5$ and decreases in the interval $0.5 \leq \lambda < 1$. In terms of both *EARL* and ARL_1 values, from small-to-moderate, moderate-to-large as well as from small-to-large shifts, the HWMA $\bar{X}^*$ scheme performs better for small shifts. For instance, when

$\gamma = 0.2$, with $r = 1$ and $\delta = 0.75$, the HWMA $\bar{X}^*$ scheme is expected to give the first signal on the 15th ($ARL_1 = 15.27$), 29th ($ARL_1 = 29.14$) and 88th ($ARL_1 = 88.55$) subgroups when $\lambda = 0.1$, 0.5 and 0.9, respectively – see Table 1. This pattern holds for the *EARL*s which show that as λ increase, the performance of the HWMA $\bar{X}^*$ scheme deteriorates.

- Stated differently, the cluster of line graphs in Figures 1(a) and (b) with smaller *ARL*s corresponds to λ = 0.1, while those with larger *ARL*s corresponds to λ = 0.9. Moreover, for each cluster of line graphs in Figures 1(a) and (b), the smaller the value of γ, the lower are the *ARL* profiles as compared to those with higher values of γ. In summary, the smaller the values of λ and γ, the better is the performance of the HWMA $\bar{X}^*$ scheme.
- As λ increases, the IC *SDRL* values increase towards the nominal ARL_0 value. The sensitivity pattern of the OOC *SDRL* ($SDRL_1$) profile in Table 2 is similar to the one of the ARL_1 profile with respect to λ and r, where it is shown that whenever λ increases, the $SDRL_1$ increase and when r increases, the $SDRL_1$ is reduced. Hence, moving forth, the focus will mainly be on the *ARL* profiles.
- Multiple measurements have a positive impact on the sensitivity of the HWMA $\bar{X}^*$ scheme. For instance, for (λ, γ) = (0.9, 0.9) and $\delta = 0.25$, the ARL_1 is equal to 416.4 and 378.8 when $r = 1$ and 4, respectively. This indicates that a multiple measurements strategy reduces the effect of measurement errors.
- Keeping in mind that the *EARL* is a weighted sum of the *ARL* (see Equation (12)), hence, as r increases, the *ARL*s decrease and thus, *EARL* also decreases; see Figure 2. Note that the *EARL* values shown at the bottom of Table 1 when r = 1 and 4 are those depicted in Figure 2. Hence, for instance, for the $EARL_1$, it is observed that there is a slightly larger drop in the value of *EARL* when r increases from 1 to 2; however, increasing r further yields lower reductions in the *EARL* values as compared to r increasing from 1 to 2.

Table 1: The ARL and $EARL$ profiles for $r = 1$ (with $r = 4$ in parentheses) of the HWMA $\bar{X}^*$ scheme when $B = 1$, $\lambda \in \{0.1, 0.5, 0.9\}$ and $\gamma \in \{0, 0.2, 0.5, 0.9\}$

	$\lambda = 0.1$				$\lambda = 0.5$				$\lambda = 0.9$			
Shift	$\gamma = 0$	$\gamma = 0.2$	$\gamma = 0.5$	$\gamma = 0.9$	$\gamma = 0$	$\gamma = 0.2$	$\gamma = 0.5$	$\gamma = 0.9$	$\gamma=0$	$\gamma=0.2$	$\gamma=0.5$	$\gamma=0.9$
0.00	499.3	497.8 (502.0)	500.0 (503.6)	498.5 (501.3)	500.7	498.7 (502.5)	499.1 (501.8)	500.1 (501.8)	502.0	506.7 (508.3)	508.2 (511.7)	508.2 (512.4)
0.25	81.19	83.65 (82.57)	95.07 (85.55)	123.1 (93.04)	218.8	224.1 (218.8)	249.3 (226.3)	293.9 (242.2)	357.7	363.8 (358.1)	379.3 (362.6)	416.4 (378.9)
0.5	28.41	29.59 (28.85)	34.15 (29.98)	45.18 (33.10)	68.88	71.52 (69.17)	86.16 (73.21)	121.9 (82.61)	177.5	182.4 (178.0)	207.1 (185.5)	259.1 (202.3)
0.75	14.90	15.27 (15.00)	17.89 (15.60)	24.11 (17.28)	27.89	29.14 (28.15)	36.22 (29.93)	54.92 (34.48)	85.05	88.55 (86.23)	107.3 (91.2)	147.7 (102.6)
1.00	9.34	9.65 (9.39)	11.21 (9.81)	15.11 (10.83)	14.16	14.68 (14.32)	18.18 (15.12)	28.38 (17.49)	43.13	45.55 (43.84)	57.01 (46.72)	87.31 (54.30)
1.25	6.54	6.76 (6.60)	7.77 (6.87)	10.54 (7.57)	8.44	8.79 (8.49)	10.83 (9.00)	16.79 (10.42)	23.58	24.98 (23.97)	32.12 (25.72)	52.28 (30.54)
1.5	5.00	5.09 (5.01)	5.87 (5.19)	7.82 (5.69)	5.65	5.86 (5.71)	7.17 (6.05)	10.89 (6.89)	13.74	14.62 (14.05)	19.39 (15.13)	32.56 (18.26)
1.75	4.00	4.10 (4.00)	4.67 (4.14)	6.15 (4.54)	4.11	4.29 (4.17)	5.16 (4.38)	7.65 (4.98)	8.64	9.19 (8.74)	12.05 (9.47)	21.00 (11.49)
2.00	3.33	3.41 (3.34)	3.87 (3.46)	5.05 (3.77)	3.20	3.31 (3.23)	3.95 (3.37)	5.74 (3.81)	5.77	6.10 (5.88)	8.17 (6.31)	14.17 (7.69)
2.25	2.83	2.90 (2.85)	3.29 (2.96)	4.25 (3.20)	2.61	2.70 (2.63)	3.16 (2.73)	4.51 (3.05)	4.11	4.33 (4.16)	5.69 (4.45)	9.91 (5.34)
2.5	2.45	2.53 (2.47)	2.86 (2.56)	3.66 (2.78)	2.20	2.26 (2.21)	2.64 (2.30)	3.68 (2.55)	3.07	3.25 (3.09)	4.16 (3.31)	7.21 (3.94)
2.75	2.14	2.20 (2.15)	2.50 (2.22)	3.23 (2.44)	1.90	1.96 (1.92)	2.23 (1.98)	3.09 (2.19)	2.40	2.53 (2.45)	3.20 (2.61)	5.41 (3.05)
3.00	1.88	1.93 (1.89)	2.22 (1.96)	2.87 (2.15)	1.68	1.72 (1.69)	1.97 (1.76)	2.64 (1.91)	1.98	2.05 (1.99)	2.56 (2.11)	4.22 (2.45)
$EARL_1$	33.46	34.54 (33.95)	39.58 (35.24)	51.89 (38.56)	82.42	84.87 (82.60)	97.46 (86.13)	124.8 (94.18)	165.9	170.1 (166.5)	187.7 (171.5)	227.6 (184.5)
$EARL_2$	4.72	4.84 (4.74)	5.55 (4.91)	7.39 (5.39)	5.35	5.56 (5.40)	6.78 (5.70)	10.27 (6.52)	12.93	13.72 (13.16)	17.93 (14.16)	30.00 (17.00)
$EARL_3$	2.33	2.39 (2.34)	2.72 (2.42)	3.50 (2.64)	2.10	2.16 (2.11)	2.50 (2.19)	3.48 (2.43)	2.89	3.04 (2.92)	3.90 (3.12)	6.69 (3.69)
$EARL_4$	19.09	19.69 (19.34)	22.56 (20.07)	29.64 (21.98)	43.89	45.22 (44.00)	52.12 (45.92)	67.52 (50.35)	89.39	91.90 (89.85)	102.8 (92.82)	128.8 (100.8)
$EARL_5$	3.52	3.62 (3.54)	4.13 (3.67)	5.45 (4.02)	3.72	3.86 (3.76)	4.64 (3.95)	6.87 (4.48)	7.91	8.38 (8.04)	10.92 (8.64)	18.35 (10.35)
$EARL_6$	13.5	13.92 (13.68)	15.95 (14.19)	20.93 (15.53)	29.96	30.86 (30.04)	35.58 (31.34)	46.17 (34.38)	60.56	62.28 (60.87)	69.83 (62.92)	88.10 (68.41)
Design parameters	$L^* = 2.938$				$L^* = 3.089$				$L^* = 3.092$			

Table 2: The $SDRL$ profiles for $r = 1$ (with $r = 4$ in parentheses) of the HWMA $\bar{X}^*$ scheme when $A = 0$, $B = 1$, $\lambda \in \{0.1, 0.5, 0.9\}$ and $\gamma \in \{0, 0.2, 0.5, 0.9\}$

	$\lambda = 0.1$				$\lambda = 0.5$				$\lambda = 0.9$			
Shift	$\gamma=0$	$\gamma=0.2$	$\gamma=0.5$	$\gamma=0.9$	$\gamma=0$	$\gamma=0.2$	$\gamma=0.5$	$\gamma=0.9$	$\gamma=0$	$\gamma=0.2$	$\gamma=0.5$	$\gamma=0.9$
0.00	407.9	406.2 (408.0)	409.0 (407.4)	407.1 (407.1)	496.1	496.0 (496.5)	500.7 (500.7)	496.6 (497.2)	504.8	503.6 (502.4)	502.0 (501.2)	504.8 (503.2)
0.25	56.65	58.89 (57.62)	68.20 (59.71)	89.08 (66.17)	214.9	220.7 (215.4)	245.6 (221.5)	291.8 (239.7)	357.4	363.6 (360.5)	381.5 (361.2)	416.3 (378.0)

0.5	17.66	18.38 (18.00)	21.74 (18.70)	29.39 (20.76)	65.73	67.56 (64.96)	82.55 (69.64)	117.7 (78.40)	176.3	181.5 (176.5)	205.5 (184.7)	259.0 (201.2)
0.75	8.69	9.01 (8.79)	10.67 (9.14)	14.57 (10.30)	24.61	25.72 (24.95)	32.81 (26.43)	51.15 (31.03)	83.95	87.46 (85.37)	103.5 (90.29)	147.7 (102.6)
1.00	5.18	5.37 (5.15)	6.27 (5.51)	8.80 (6.10)	11.57	11.93 (11.57)	15.31 (12.38)	24.99 (14.60)	42.41	45.04 (43.13)	55.98 (46.36)	86.38 (53.60)
1.25	3.42	3.53 (3.44)	4.17 (3.61)	5.91 (4.06)	6.30	6.58 (6.31)	8.40 (6.86)	13.96 (8.04)	22.84	24.26 (23.20)	31.33 (24.94)	51.20 (29.60)
1.5	2.44	2.51 (2.46)	3.01 (2.57)	4.23 (2.89)	3.78	4.00 (3.86)	5.13 (4.20)	8.52 (4.89)	12.96	13.82 (13.21)	18.67 (14.32)	31.90 (17.39)
1.75	1.86	1.92 (1.87)	2.25 (1.96)	3.18 (2.19)	2.53	2.70 (2.60)	3.39 (2.76)	5.55 (3.25)	7.85	8.40 (8.02)	11.20 (8.70)	20.21 (10.74)
2.00	1.52	1.57 (1.54)	1.80 (1.59)	2.48 (1.73)	1.83	1.91 (1.83)	2.41 (1.95)	3.90 (2.29)	5.01	5.35 (5.13)	7.38 (5.60)	13.42 (6.92)
2.25	1.32	1.35 (1.33)	1.51 (1.37)	2.01 (1.47)	1.37	1.44 (1.39)	1.78 (1.47)	2.88 (1.71)	3.38	3.57 (3.40)	4.93 (3.71)	9.11 (4.56)
2.5	1.20	1.22 (1.20)	1.33 (1.23)	1.71 (1.31)	1.08	1.13 (1.10)	1.39 (1.16)	2.20 (1.32)	2.34	2.50 (2.35)	3.42 (2.59)	6.45 (3.21)
2.75	1.10	1.12 (1.11)	1.22 (1.12)	1.49 (1.19)	0.88	0.92 (0.90)	1.12 (0.95)	1.72 (1.07)	1.69	1.80 (1.73)	2.46 (1.89)	4.65 (2.32)
3.00	1.00	1.02 (1.01)	1.11 (1.04)	1.33 (1.10)	0.74	0.78 (0.75)	0.92 (0.79)	1.40 (0.90)	1.26	1.34 (1.28)	1.85 (1.41)	3.47 (1.72)
Design parameters	***L* = 2.938**				***L* = 3.089**				***L* = 3.092**			

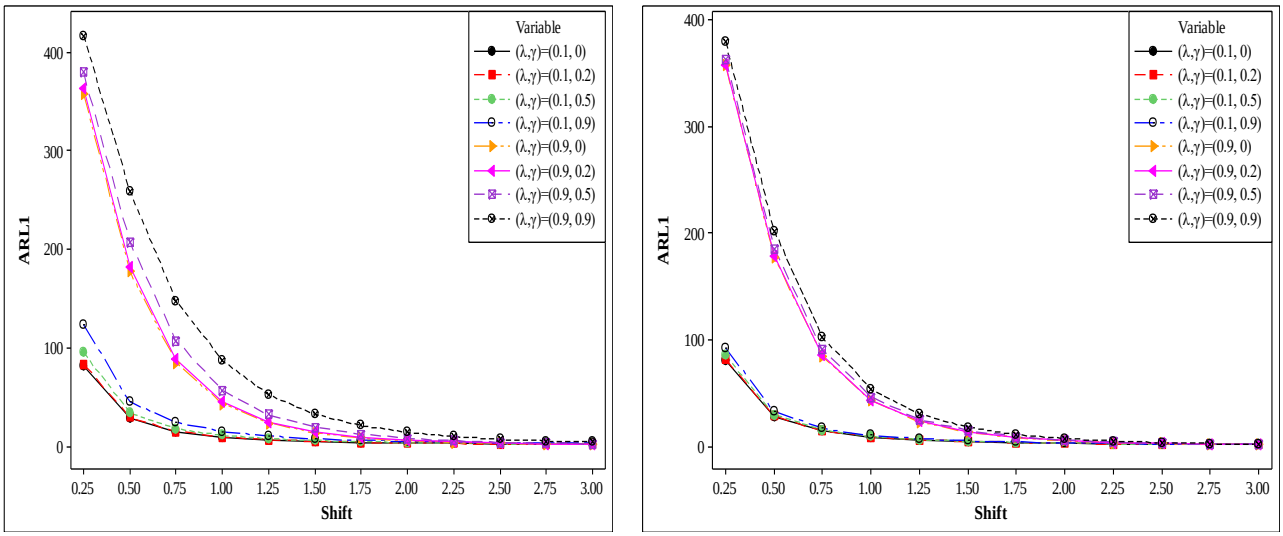

(a) ARL_1 profile when $\lambda = 0.1$ & 0.9 and $r = 1$ (b) ARL_1 profile when $\lambda = 0.1$ & 0.9 and $r = 4$

Figure 1: The ARL_1 profiles for $r = 1$ & 4 of the HWMA $\bar{X}^*$ scheme when $\gamma \in \{0, 0.2, 0.5, 0.9\}$ and $\lambda \in \{0.1, 0.9\}$

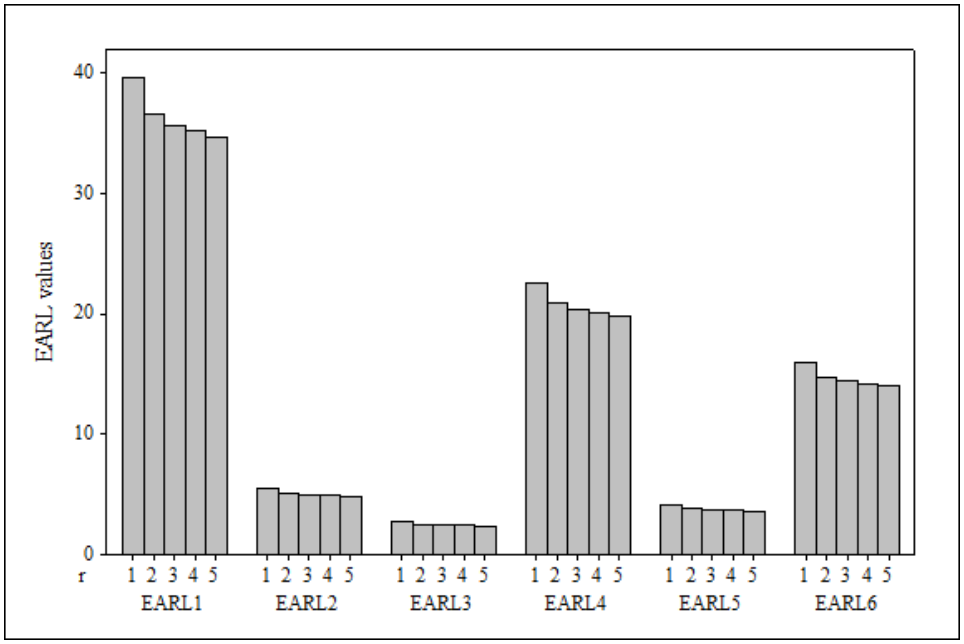

Figure 2: The *EARL* profiles of the HWMA $\bar{X}^*$ scheme for $r \in \{1, 2, 3, 4, 5\}$ when $\gamma = 0.5$, $n = 5$, $\lambda = 0.1$ and L^*=2.9380

It is worth mentioning that varying A yields no effect on the *ARL* and *SDRL* profiles of the HWMA $\bar{X}^*$ scheme and that B is equal to 1 in Tables 1 and 2 as well as in Figures 1 and 2. Next, in Table 3, the effect of varying B is illustrated. Firstly, when γ=0, the *ARL* profiles are the same for any integer value of B (i.e. $\forall B$). Secondly, for $\gamma > 0$, it is shown in Table 3 that for $\delta > 0$, the *ARL* and *EARL* decrease as B increases. That is, as B increases, there is a reduction in the negative effect of measurement errors. Thirdly, it is also shown in Table 3 that the *ARL*s and *EARL*s are lower when r=4 than those when r=1, indicating a reduction in the negative effect of measurement errors as r increases. Finally, although Table 3 is illustrated for λ=0.1 and n=5 only, this pattern holds for other values of λ and n, whenever $\gamma > 0$ and $\delta > 0$. Note that a significant reduction is observed for large values of γ, e.g. for $\gamma = 0.9$ with $\delta = 0.25$ and $r = 1$, the ARL_1 is equal to 122.2, 93.34 and 86.58 when B is equal to 1, 2 and 3, respectively. A similar pattern is observed for *EARL*s.

Table 3.The effect of B on the *ARL* and *EARL* for r=1 (with r=4 in parentheses) of the HWMA $\bar{X}^*$ scheme when $B \in \{1, 2, 3\}$, λ=0.1, L^*=2.9380, $\gamma \in \{0, 0.2, 0.5, 0.9\}$, n = 5, a nominal ARL_0 value of 500

	$\gamma = 0$	$\gamma = 0.2$			$\gamma = 0.5$			$\gamma = 0.9$		
Shift	$\forall B$	$B = 1$	$B = 2$	$B = 3$	$B = 1$	$B = 2$	$B = 3$	$B = 1$	$B = 2$	$B = 3$
0.00	500.7	501.9 (502.3)	498.6 (501.6)	501.3 (503.2)	502.0 (502.8)	498.4 (499.6)	499.2 (501.6)	500.6 (502.5)	501.6 (500.1)	502.2 (499.0)
0.25	81.87	83.77 (82.24)	82.21 (81.97)	82.09 (81.59)	95.69 (85.40)	85.33 (82.83)	83.45 (81.90)	122.2 (93.36)	93.34 (83.88)	86.58 (82.94)
0.50	28.76	29.43 (28.77)	28.79 (28.73)	28.52 (28.51)	33.85 (29.95)	30.03 (28.98)	29.17 (28.78)	45.41 (32.90)	33.04 (29.75)	30.50 (29.12)
0.75	14.93	15.34 (15.01)	14.94 (14.95)	14.90 (14.93)	17.87 (15.60)	15.61 (15.09)	15.20 (14.94)	24.01 (17.26)	17.37 (15.49)	15.93 (15.17)
1.00	9.29	9.63 (9.43)	9.42 (9.35)	9.38 (9.30)	11.14 (9.76)	9.79 (9.46)	9.58 (9.38)	15.13 (10.82)	10.83 (9.74)	10.03 (9.48)
1.25	6.56	6.71 (6.60)	6.59 (6.56)	6.58 (6.56)	7.81 (6.88)	6.86 (6.61)	6.66 (6.58)	10.49 (7.55)	7.56 (6.80)	7.01 (6.63)
1.50	4.96	5.12 (5.01)	5.01 (5.00)	5.00 (4.97)	5.85 (5.19)	5.19 (5.02)	5.09 (5.00)	7.84 (5.72)	5.70 (5.16)	5.29 (5.07)
1.75	3.98	4.10 (4.02)	4.01 (3.99)	3.99 (3.99)	4.69 (4.15)	4.17 (4.02)	4.07 (4.00)	6.14 (4.54)	4.55 (4.12)	4.24 (4.04)
2.00	3.32	3.42 (3.34)	3.35 (3.32)	3.32 (3.33)	3.86 (3.45)	3.46 (3.35)	3.38 (3.33)	5.03 (3.77)	3.77 (3.44)	3.52 (3.37)
2.25	2.82	2.91 (2.85)	2.86 (2.83)	2.85 (2.83)	3.29 (2.95)	2.95 (2.86)	2.88 (2.84)	4.23 (3.20)	3.21 (2.92)	3.00 (2.88)
2.50	2.45	2.52 (2.48)	2.46 (2.45)	2.46 (2.45)	2.86 (2.55)	2.56 (2.48)	2.48 (2.47)	3.67 (2.78)	2.78 (2.53)	2.59 (2.48)
2.75	2.13	2.21 (2.16)	2.15 (2.14)	2.15 (2.14)	2.51 (2.24)	2.24 (2.16)	2.18 (2.15)	3.21 (2.44)	2.43 (2.21)	2.27 (2.18)
3.00	1.88	1.94 (1.88)	1.88 (1.88)	1.88 (1.87)	2.22 (1.96)	1.96 (1.89)	1.91 (1.88)	2.87 (2.16)	2.15 (1.96)	2.00 (1.90)
$EARL_1$	33.71	34.54 (33.86)	33.83 (33.75)	33.73 (33.58)	39.64 (35.18)	35.19 (34.09)	34.35 (33.75)	51.69 (38.59)	38.65 (34.72)	35.76 (34.18)
$EARL_2$	4.71	4.84 (4.74)	4.74 (4.72)	4.72 (4.71)	5.55 (4.92)	4.92 (4.75)	4.80 (4.72)	7.38 (5.40)	5.40 (4.88)	5.02 (4.78)
$EARL_3$	2.32	2.40 (2.34)	2.34 (2.33)	2.34 (2.32)	2.72 (2.43)	2.43 (2.35)	2.36 (2.34)	3.50 (2.65)	2.64 (2.41)	2.47 (2.36)
$EARL_4$	19.21	19.69 (19.30)	19.29 (19.23)	19.23 (19.15)	22.60 (20.05)	20.06 (19.42)	19.58 (19.24)	29.53 (21.99)	22.02 (19.80)	20.39 (19.48)
$EARL_5$	4.15	4.28 (4.20)	4.19 (4.17)	4.18 (4.16)	4.91 (4.35)	4.35 (4.21)	4.25 (4.18)	6.51 (4.78)	4.78 (4.32)	4.44 (4.23)
$EARL_6$	13.58	13.93 (13.65)	13.64 (13.60)	13.60 (13.54)	15.97 (14.17)	14.18 (13.73)	13.84 (13.60)	20.85 (15.54)	15.56 (14.00)	14.41 (13.77)

With regard to the linearly increase in the variance, the effect of varying B, C and D is investigated in Table 4. Note that for B=2, only C=0 is shown to preserve writing space. Firstly, for B=1, D=1 and δ=0.25, the ARL_1 is equal to 131.2, 169.7 and 200.4 when C is equal to 0, 1 and 2, respectively. A similar pattern is observed for the corresponding *EARL*s. This shows that when C increases there is deterioration in the performance of the HWMA $\bar{X}^*$ scheme. Secondly, for B=1, C=0 and δ=0.25, the ARL_1 is equal to

131.2, 169.8 and 200.3 when D is equal to 1, 2 and 3, respectively. A similar pattern is observed for the corresponding *EARL*s. This shows that when D increases there is a deterioration in the performance of the HWMA $\bar{X}^*$ scheme. Thirdly, for C=0, D=1 and δ=0.25, the ARL_1 is equal to 131.2 when B=1; however, it is equal to 95.2 when B=2. Similarly, the *EARL*s also decreases when B increases. This shows that for a fixed C and D, increasing B yields an improved performance for the HWMA $\bar{X}^*$ scheme, which implies that there is a reduction in the negative effect of measurement errors. Finally, it is shown in Table 4 that the *ARL*s and *EARL*s are lower when r=4 than those when r=1 indicating a reduction in the negative effect of measurement errors as r increases.

Table 4: The ARL and $EARL$ profiles for $r = 1$ (with $r = 4$ in parentheses) of the HWMA $\bar{X}^*$ scheme when $B \in \{1, 2\}$, $C \in \{0, 1, 2\}$, $D \in \{1, 2, 3\}$ and $\lambda \in \{0.1, 0.5, 0.9\}$

	B = 1									B = 2		
	C = 0			C = 1			C = 2			C = 0		
Shift	D = 1	D = 2	D = 3	D = 1	D = 2	D = 3	D = 1	D = 2	D = 3	D = 1	D = 2	D = 3
0.00	500.8 (501.0)	501.4 (504.1)	502.9 (501.1)	497.5 (500.9)	502.5 (501.9)	498.6 (500.1)	502.7 (502.8)	500.2 (499.7)	502.5 (498.3)	500.3 (504.7)	497.5 (501.6)	498.4 (499.5)
0.25	131.2 (95.63)	169.8 (108.5)	200.3 (119.8)	169.7 (108.4)	200.2 (120.0)	224.3 (130.9)	200.4 (120.0)	224.6 (131.2)	245.8 (142.0)	95.3 (85.4)	108.6 (88.6)	119.6 (92.6)
0.5	48.77 (34.03)	66.21 (39.16)	81.54 (44.25)	66.22 (39.27)	81.77 (44.29)	95.47 (48.88)	81.61 (44.20)	96.33 (48.83)	107.9 (53.51)	33.96 (30.10)	39.24 (31.46)	43.91 (32.58)
0.75	26.10 (17.83)	35.88 (20.68)	44.64 (23.41)	35.73 (20.77)	44.64 (23.42)	52.78 (25.94)	44.57 (23.33)	52.80 (26.05)	60.82 (28.57)	17.84 (15.69)	20.74 (16.41)	23.37 (17.06)
1.00	16.37 (11.17)	22.74 (12.97)	28.48 (14.71)	22.76 (12.97)	28.58 (14.77)	34.04 (16.39)	28.46 (14.68)	33.91 (16.38)	39.30 (18.06)	11.17 (9.80)	12.93 (10.23)	14.71 (10.74)
1.25	11.38 (7.81)	15.86 (8.99)	19.94 (10.23)	15.88 (9.03)	20.00 (10.20)	23.86 (11.36)	19.99 (10.23)	23.85 (11.39)	27.83 (12.58)	7.78 (6.89)	8.98 (7.20)	10.24 (7.53)
1.5	8.50 (5.86)	11.73 (6.75)	14.83 (7.62)	11.71 (6.75)	14.79 (7.64)	17.86 (8.50)	14.90 (7.61)	17.86 (8.50)	20.64 (9.33)	5.84 (5.20)	6.77 (5.42)	7.65 (5.67)
1.75	6.67 (4.67)	9.18 (5.34)	11.58 (5.99)	9.16 (5.32)	11.59 (5.97)	13.92 (6.65)	11.56 (5.98)	13.93 (6.63)	16.13 (7.28)	4.67 (4.16)	5.35 (4.33)	6.00 (4.51)
2.00	5.41 (3.87)	7.41 (4.39)	9.31 (4.89)	7.41 (4.38)	9.27 (4.92)	11.20 (5.41)	9.35 (4.92)	11.14 (5.41)	12.95 (5.93)	3.86 (3.45)	4.40 (3.59)	4.92 (3.74)
2.25	4.57 (3.30)	6.16 (3.72)	7.76 (4.15)	6.16 (3.72)	7.73 (4.15)	9.23 (4.56)	7.73 (4.16)	9.18 (4.56)	10.76 (4.98)	3.29 (2.95)	3.73 (3.06)	4.13 (3.18)

2.5	3.93 (2.87)	5.26 (3.23)	6.55 (3.57)	5.26 (3.22)	6.55 (3.58)	7.79 (3.93)	6.51 (3.59)	7.79 (3.92)	9.05 (4.25)	2.86 (2.55)	3.23 (2.66)	3.59 (2.76)
2.75	3.45 (2.49)	4.57 (2.84)	5.66 (3.15)	4.58 (2.85)	5.65 (3.14)	6.71 (3.45)	5.68 (3.14)	6.73 (3.45)	7.75 (3.72)	2.50 (2.24)	2.84 (2.32)	3.15 (2.43)
3.00	3.06 (2.21)	4.04 (2.52)	4.95 (2.80)	4.04 (2.53)	4.97 (2.80)	5.87 (3.07)	4.97 (2.80)	5.87 (3.06)	6.77 (3.32)	2.21 (1.97)	2.51 (2.04)	2.80 (2.13)
$\boldsymbol{EARL_1}$	55.60 (39.67)	73.66 (45.32)	88.74 (50.54)	73.59 (45.35)	88.80 (50.63)	101.7 (55.54)	88.77 (50.56)	101.9 (55.61)	113.4 (60.54)	39.57 (35.26)	45.37 (36.68)	50.39 (38.24)
$\boldsymbol{EARL_2}$	7.99 (5.55)	11.05 (6.37)	13.92 (7.18)	11.04 (6.37)	13.91 (7.18)	16.71 (7.98)	13.95 (7.19)	16.70 (7.98)	19.39 (8.78)	5.54 (4.93)	6.38 (5.14)	7.20 (5.36)
$\boldsymbol{EARL_3}$	3.75 (2.72)	5.01 (3.08)	6.23 (3.42)	5.01 (3.08)	6.23 (3.42)	7.40 (3.75)	6.22 (3.42)	7.39 (3.75)	8.58 (4.07)	2.72 (2.43)	3.08 (2.52)	3.42 (2.63)
$\boldsymbol{EARL_4}$	31.79 (22.61)	42.35 (25.84)	51.33 (28.86)	42.32 (25.86)	51.36 (28.91)	59.19 (31.76)	51.36 (28.87)	59.30 (31.80)	66.41 (34.66)	22.56 (20.09)	25.87 (20.91)	28.79 (21.80)
$\boldsymbol{EARL_5}$	7.04 (4.92)	9.66 (5.64)	12.12 (6.35)	8.03 (4.73)	10.07 (5.30)	12.06 (5.87)	12.13 (6.35)	14.47 (7.03)	16.80 (7.72)	4.91 (4.36)	5.64 (4.54)	6.35 (4.74)
$\boldsymbol{EARL_6}$	22.45 (15.98)	29.91 (18.25)	36.29 (20.38)	29.88 (18.27)	36.31 (20.41)	41.93 (22.42)	36.31 (20.39)	42.00 (22.45)	47.14 (24.46)	15.94 (14.20)	18.27 (14.78)	20.34 (15.41)

Figure 3 displays the percentage decrease (*%Decrease*) in the performance of the HWMA $\bar{X}^*$ scheme with respect to γ for different values of λ; while Figure 4 displays the *%Increase* in the ARL_1 profile of the HWMA $\bar{X}^*$ scheme from using one set of measurements (i.e., $r = 1$) to multiple sets of measurements (i.e., $r > 1$). Moreover, Figure 5 displays the expected *%Decrease* in the performance of the HWMA $\bar{X}^*$ scheme for different γ values. The *%Decrease* and the *expected %Decrease* in the performance are computed using the following formula:

$$\%Decrease(\delta) = \frac{ARL_1(\delta) - ARL_1^*(\delta)}{ARL_1^*(\delta)} \times 100 \tag{13}$$

and

$$Expected\ \%Decrease = \frac{1}{\Delta} \sum_{\delta=\delta_{min}}^{\delta_{max}} \%Decrease(\delta), \tag{14}$$

where $ARL_1(\delta)$ is the OOC *ARL* value of the HWMA $\bar{X}^*$ scheme for a specific shift (δ) when $\gamma \neq 0$ and $ARL_1^*(\delta)$ is the OOC *ARL* value for a specific shift when $\gamma = 0$.

From Figures 3 (a)-(c), it can be seen that the *%Decrease* in the performance of the HWMA $\bar{X}^*$ scheme is larger (smaller) for large (small) values of γ. Moreover, the *%Decrease* in the performance is larger for very small shifts when λ is small; however, it is smaller for moderate and large values of δ when λ is small and the converse is true for large values of λ. The *%Decrease* in the performance of the HWMA $\bar{X}^*$ scheme reaches its maximum point when $\delta = 1$ for moderate values of λ and δ=1.75 for large values of λ. However, the minimum point is attained for very small shift values. Note that for small values of λ, the *%Decrease* in the performance of the HWMA $\bar{X}^*$ scheme reaches its maximum point in the interval $0 < \delta < 0.25$.

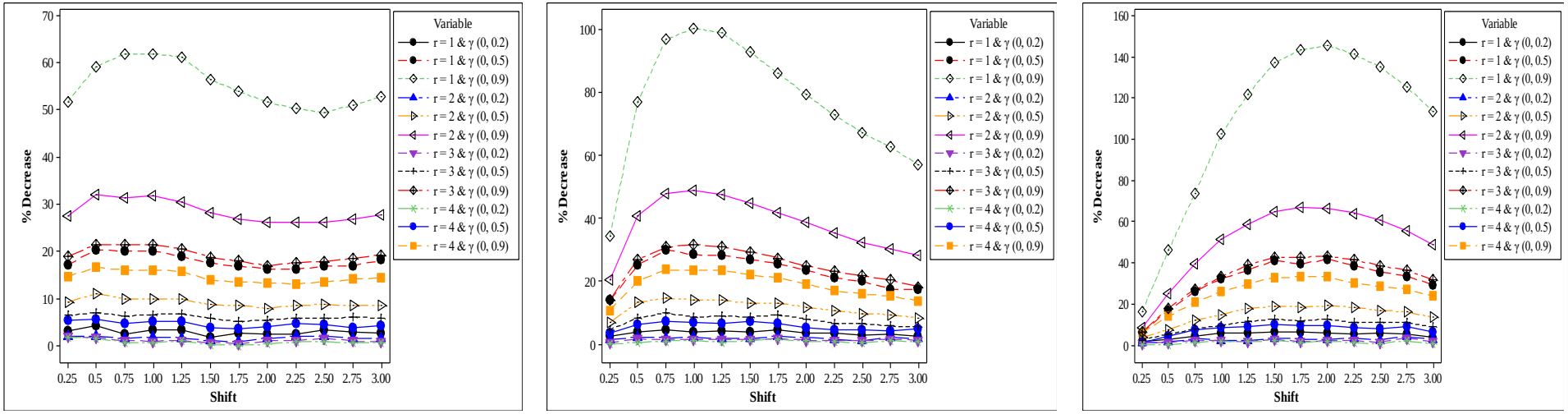

(a) $\lambda = 0.1$ (b) $\lambda = 0.5$ (c) $\lambda = 0.9$

Figure 3: The *%Decrease* in the ARL_1 profile of the HWMA $\bar{X}^*$ scheme with a constant variance for different values of γ and λ

The *%Increase* and the *expected %Increase* in the performance can also be computed in a similar way using the following formula:

$$\%Increase(\delta) = \left|\frac{ARL_1(\delta) - ARL_1^*(\delta)}{ARL_1^*(\delta))}\right| \times 100 \tag{15}$$

and

$$Expected\ \%Increase = \frac{1}{\Delta}\sum_{\delta=\delta_{min}}^{\delta_{max}} \%Increase(\delta), \tag{16}$$

where $ARL_1(\delta)$ is the OOC *ARL* value of the HWMA $\bar{X}^*$ scheme for a specific shift (δ) when $r > 1$ and $ARL_1^*(\delta)$ is the OOC *ARL* value for a specific shift when $r = 1$.

Figure 4 shows that for small-to-large shifts, the *%Increase* in the performance or sensitivity of the HWMA $\bar{X}^*$ scheme increases as r increases. For instance, a small shift of size 0.25 with $\gamma = 0.5$ and $\lambda = 0.1$, there is a *%Increase* of 6.68%, 9.17% and 10.01% when $r = 2$, 3 and 4, respectively. The larger the value of γ, the higher the *%Increase* in the sensitivity of the HWMA $\bar{X}^*$ scheme. It can also be observed that for small values of γ there are random patterns in the *%Increase ARL* function.

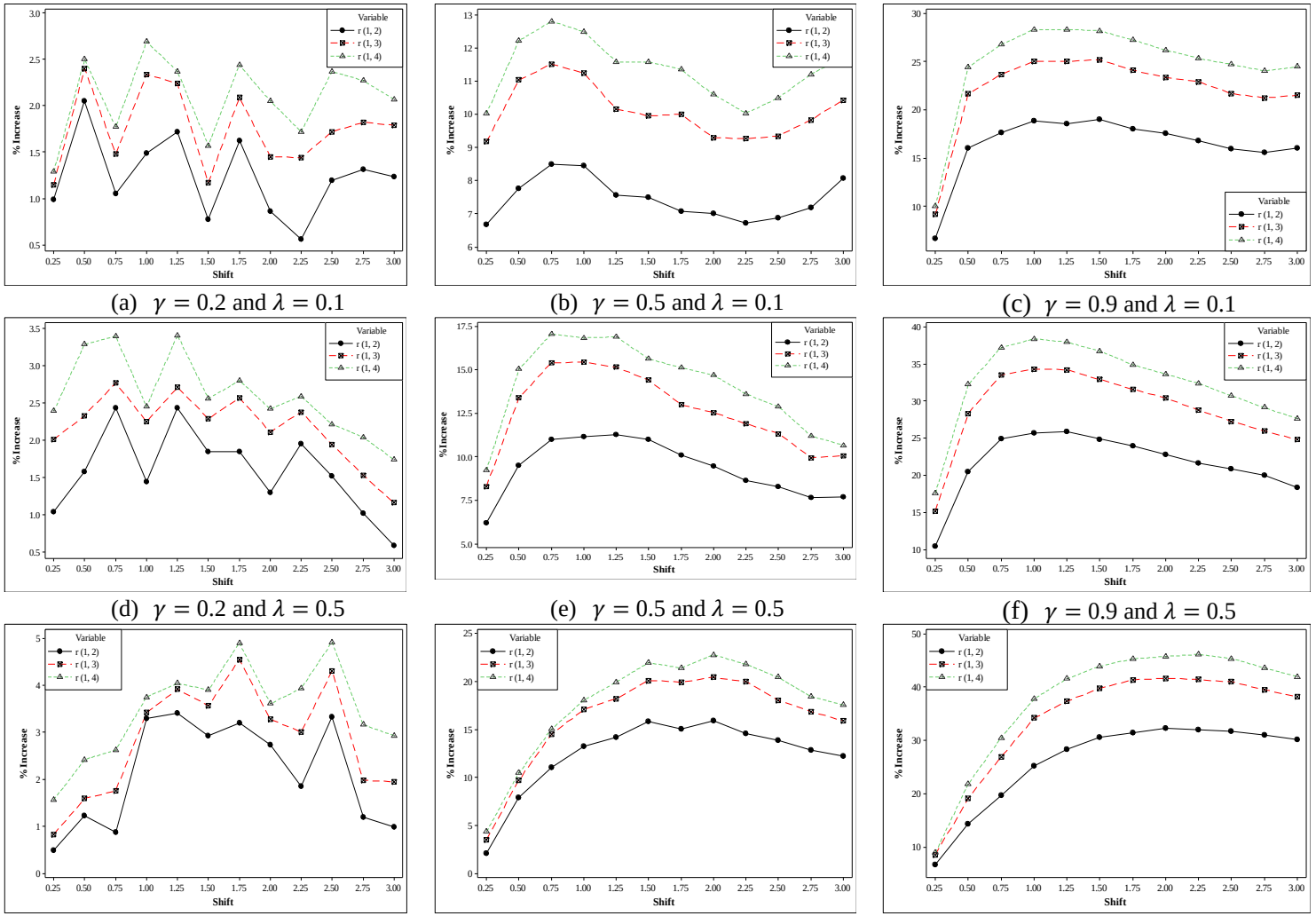

(a) $\gamma = 0.2$ and $\lambda = 0.1$ (b) $\gamma = 0.5$ and $\lambda = 0.1$ (c) $\gamma = 0.9$ and $\lambda = 0.1$

(d) $\gamma = 0.2$ and $\lambda = 0.5$ (e) $\gamma = 0.5$ and $\lambda = 0.5$ (f) $\gamma = 0.9$ and $\lambda = 0.5$

(g) $\gamma = 0.2$ and $\lambda = 0.9$ (h) $\gamma = 0.5$ and $\lambda = 0.9$ (i) $\gamma = 0.9$ and $\lambda = 0.9$

Figure 4: The *%Increase* in the ARL_1 profile of the HWMA $\bar{X}^*$ scheme with a constant variance for different values of γ and $\lambda = 0.1$

Figures 5(a)-(l) show that when λ = 0.1 (i.e. small) and $r = 1$, then for small shifts in the process mean, the *expected %Decrease* in the sensitivity of the HWMA $\bar{X}^*$ scheme is 3.25%, 19.35% and 58.57% when $\gamma = 0.2$, 0.5 and 0.9, respectively. For moderate values of λ = 0.5, when $\gamma = 0.2$, 0.5 and 0.9, *the expected %Decrease* in the performance of the HWMA $\bar{X}^*$ scheme is 3.61%, 24.32% and 77.16%, respectively. However, for large value of λ = 0.9, when $\gamma = 0.2$, 0.5 and 0.9, the *expected %Decrease* in the performance of the HWMA $\bar{X}^*$ scheme is 3.55%, 19.43% and 47.68%, respectively. These results show that when $\gamma = 0.2$, 0.5 and 0.9 the *expected %Decrease* in the sensitivity varies between 3.25 to 3.61%, 19.35 to 24.32% and 47.68 to 77.16%, respectively. Thus, when $r = 2$, for $\gamma = 0.2$, 0.5 and 0.9, the *expected %Decrease* in the sensitivity of the HWMA $\bar{X}^*$ scheme varies between 1.80 to 2.01%, 9.72 to 11.97% and 27.82 to 34.92%, respectively. That is, a higher value of r yields lower *expected %Decrease* in the sensitivity of the HWMA $\bar{X}^*$ scheme as compared to a lower one.

Figures 6 (a)-(k) display the *expected %Increase* in the sensitivity of the HWMA $\bar{X}^*$ scheme for different values of r and λ. It is observed that regardless of the size of the mean shift, there is a large increase in the sensitivity of the scheme when γ is small and the *expected %Increase* is higher for large values of r. Moreover, Figure 6 shows that the larger the value of λ the more sensitive is the HWMA $\bar{X}^*$ scheme, except for small shifts in the process mean.

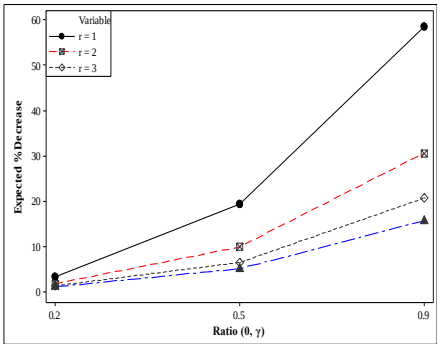

(a) $\lambda = 0.1$

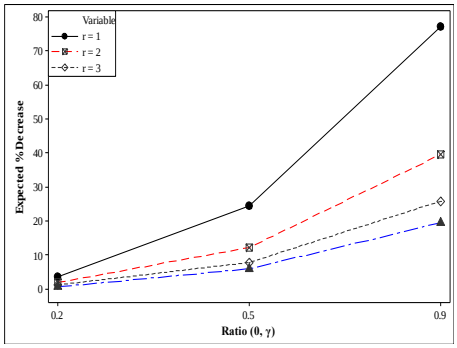

(b) $\lambda = 0.5$

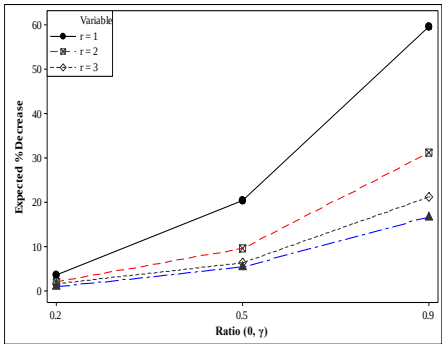

(c) $\lambda = 0.9$

Panel 1: Small shifts

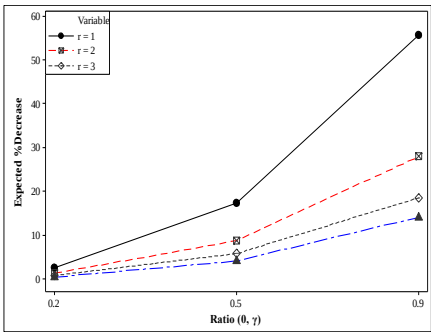

(d) $\lambda = 0.1$

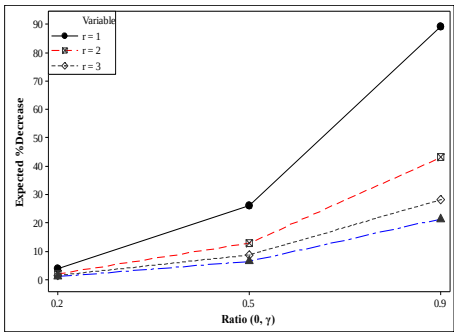

(e) $\lambda = 0.5$

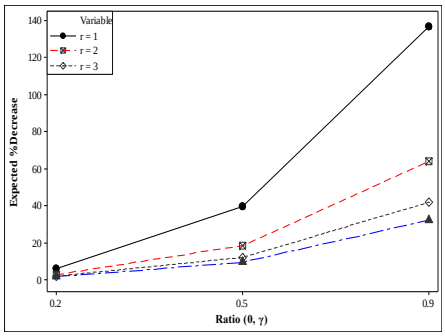

(f) $\lambda = 0.9$

Panel 2: Moderate shifts

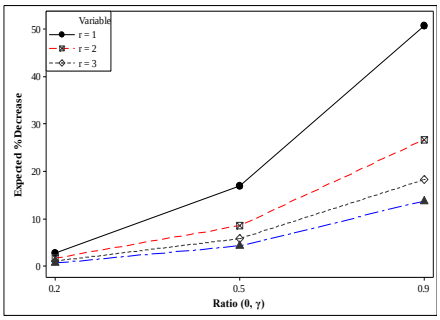

(g) $\lambda = 0.1$

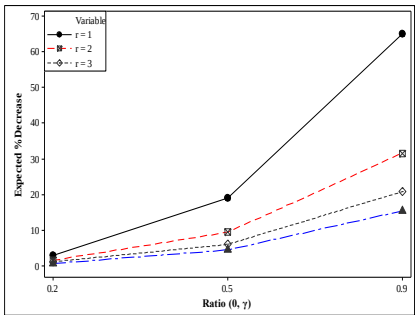

(h) $\lambda = 0.5$

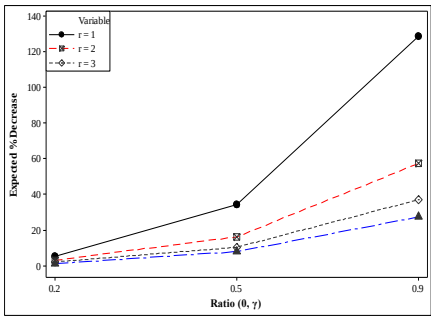

(i) $\lambda = 0.9$

Panel 3: Large shifts

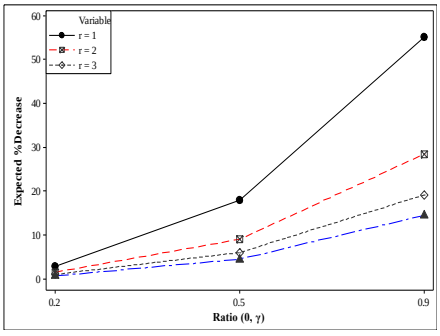

(j) $\lambda = 0.1$

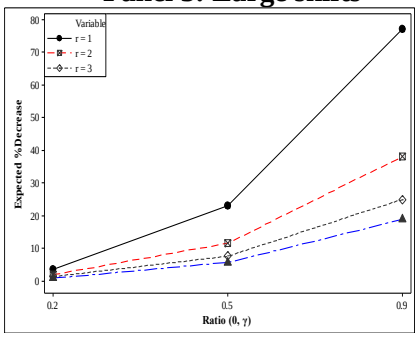

(k) $\lambda = 0.5$

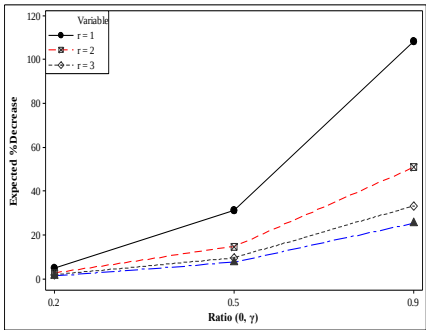

(l) $\lambda = 0.9$

Panel 4: Small to large shifts

Figure 5: The *Expected %Decrease* in the ARL_1 value of the HWMA $\bar{X}^*$ scheme with a constant variance

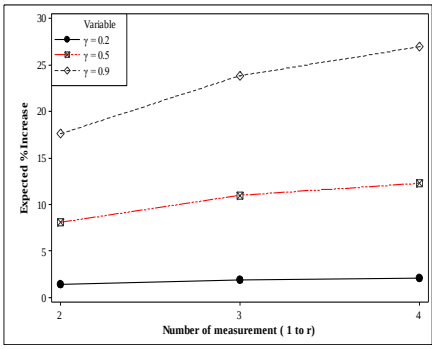

(a) $\lambda = 0.1$

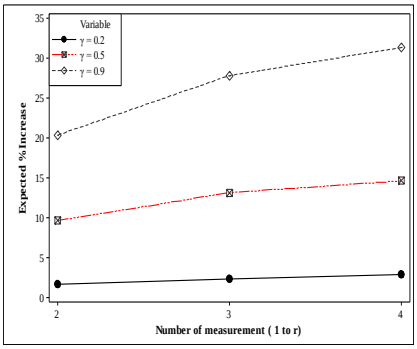

(b) $\lambda = 0.5$

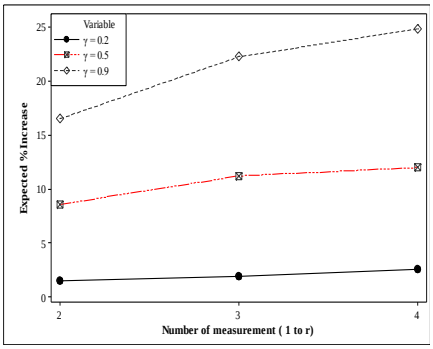

(c) $\lambda = 0.9$

Panel 1: Small shifts

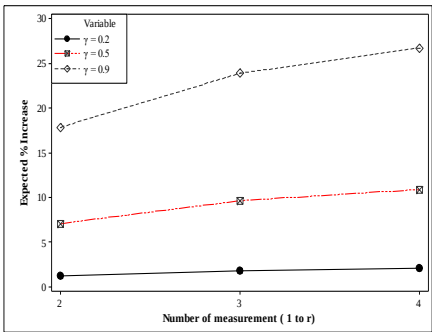

(d) $\lambda = 0.1$

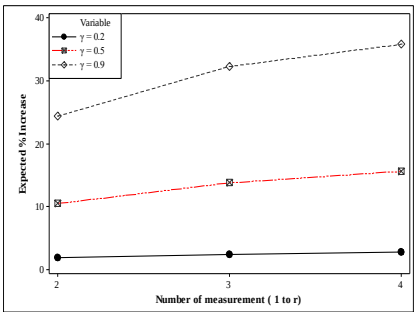

(e) $\lambda = 0.5$

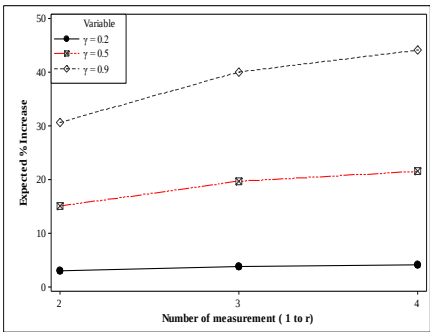

(f) $\lambda = 0.9$

Panel 2: Moderate shifts

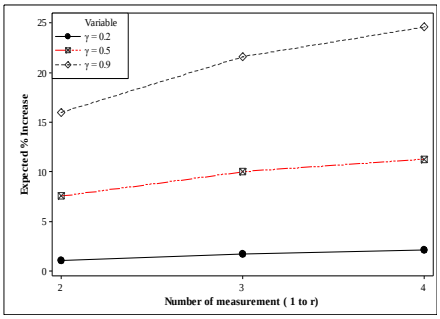

(g) $\lambda = 0.1$

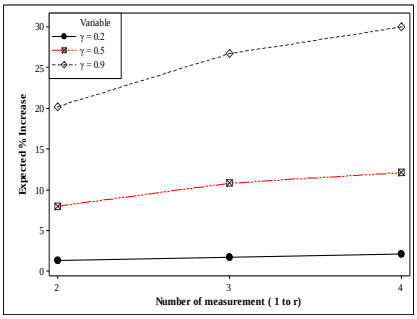

(h) $\lambda = 0.5$

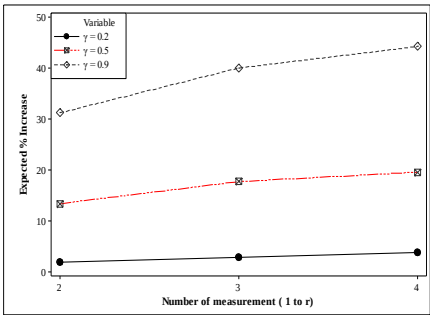

(i) $\lambda = 0.9$

Panel 3: Large shifts

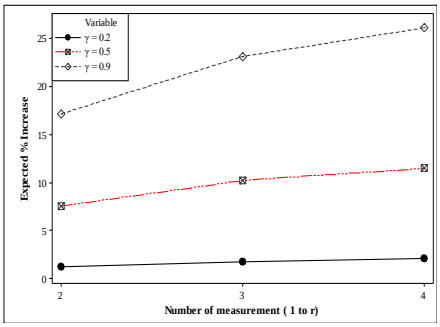

(j) $\lambda = 0.1$

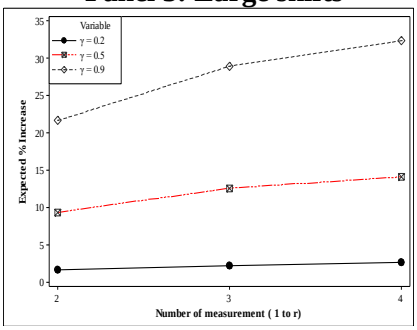

(k) $\lambda = 0.5$

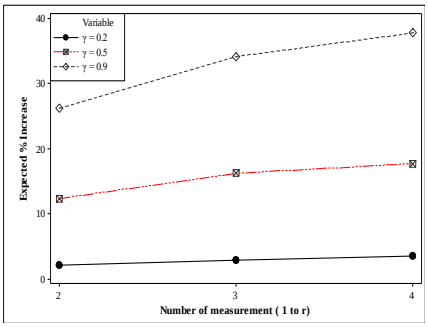

(l) $\lambda = 0.9$

Panel 4: Small to large shifts

Figure 6: The *Expected %Increase* in the ARL_1 value of the HWMA $\bar{X}^*$ scheme with a constant variance

In the design of statistical monitoring schemes with measurement errors, it is very important to investigate the number of measurements per sampling time necessary to compensate for the negative effect of measurement errors. In most of the cases, the elimination of the effect of measurement errors is almost impossible because in some situations, measurement costs need to be minimized and the use of large sample sizes must be avoided. Figure 7 presents the *marginal %Increase* in the sensitivity of the HWMA $\bar{X}^*$ scheme when using r-measurements with $\lambda = 0.1$. In this paper, the *marginal %Increase* in the performance or sensitivity is defined as a percentage drop in the ARL_1 value for one unit increase in the value of r. From Figure 7, it is observed that the *marginal %Increase* decreases as the number of measurement increases. Therefore, for small level of measurement errors, it is advised to use 3 sets of measurements of size 5 because when $r = 4$ the *marginal %increase* in the sensitivity is around 1% which is insignificant. For moderate values of γ, it is advised to use 3 or 4 sets of measurements and for large values of γ, the use of no more than 4 or 5 sets of measurements is suggested. These recommendations apply to all values of λ.

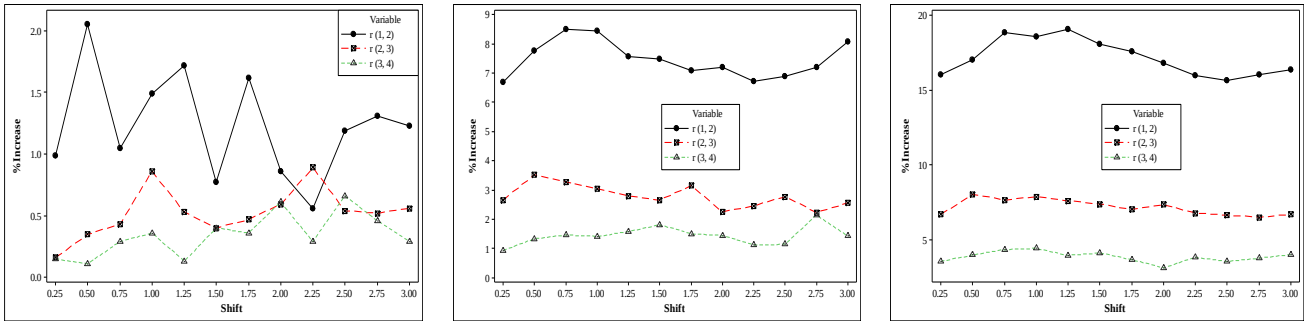

(a) $\gamma = 0.2$ (b) $\gamma = 0.5$ (c) $\gamma = 0.9$

Figure 7: *Marginal %Increases* of the HWMA $\bar{X}^*$ scheme with a constant variance when $\lambda = 0.1$

Note that Figures 3 to 7 were constructed for any A value and B=1. For other values of B, C and D, a similar conclusion is observed for different values of λ, γ and r.

Performance comparison

In this section, the HWMA $\bar{X}^*$ scheme is compared to the CUSUM and EWMA $\bar{X}^*$ schemes. The implementation of the CUSUM $\bar{X}^*$ scheme requires two important parameters known as the reference and control limits parameters denoted by k_C and h_C, respectively. However, the EWMA $\bar{X}^*$ scheme also requires two parameters known as the smoothing and control limits parameter denoted by λ_E and L_E, respectively. For a nominal ARL_0 value of 500 and $\lambda_E = 0.1$, it is observed that (k_C, h_C) = (0.125, 5.887) and $L_E = 2.824$ are such that the CUSUM and EWMA $\bar{X}^*$ schemes yield an attained IC ARL as close as possible to 500. Table 5 displays the *ARL* and *EARL* profiles of the HWMA, CUSUM and EWMA $\bar{X}^*$ schemes for different values of γ and r. From this table, at each shift value or range of shift values, the best performing scheme is boldfaced. It is observed that, regardless of the level of measurement error and the number of measurements, the HWMA scheme outperforms the CUSUM and EWMA schemes under small mean shifts. The CUSUM scheme outperforms the EWMA scheme for very small shifts (i.e., $0 < \delta \leq 0.25$) and the converse is true for shifts of size $0.25 < \delta \leq 1$. For small and moderate shifts, the EWMA scheme performs better than the CUSUM and HWMA schemes and the latter outperforms the CUSUM scheme. For small-to-moderate shifts as well as for small-to-large shifts in the process mean, the HWMA scheme is superior to the CUSUM and EWMA schemes. However, for moderate-to-large shifts, the EWMA scheme performs better than CUSUM and HWMA schemes and the latter is superior to the CUSUM scheme.

Table 5: Performance comparison of the *ARL* and *EARL* values for r=1 (with r=4 in parentheses) of the HWMA, EWMA and CUSUM $\bar{X}^*$ schemes when $\lambda = 0.1$, $\gamma \in \{0, 0.2, 0.5, 0.9\}$ for a nominal ARL_0 value of 500

Shift	CUSUM $\bar{X}^*$ scheme				EWMA $\bar{X}^*$ scheme				HWMA $\bar{X}^*$ scheme			
	$k_C = 0.125$ and $h_C = 5.887$				$L_E = 2.824$ and $\lambda = 0.1$				$L^* = 2.938$ and $\lambda = 0.1$			
	$\gamma = 0$	$\gamma = 0.2$	$\gamma = 0.5$	$\gamma = 0.9$	$\gamma = 0$	$\gamma = 0.2$	$\gamma = 0.5$	$\gamma = 0.9$	$\gamma = 0$	$\gamma = 0.2$	$\gamma = 0.5$	$\gamma = 0.9$
0.00	500.60	501.02 (502.13)	500.51 (502.70)	500.93 (503.58)	500.72	499.06 (500.55)	502.63 (501.54)	500.92 (499.52)	499.32	497.82 (501.99)	499.97 (503.58	498.50 (501.33)
0.25	84.00	85.65 (84.22)	97.14 (87.22)	123.9 (94.43)	102.69	106.50 (105.14)	124.17 (109.61)	164.75 (119.82)	**81.19**	**83.65 (82.57)**	**95.07 (85.55)**	**123.14 (93.04)**
0.50	34.66	35.43 (34.89)	39.60 (35.99)	49.68 (38.76)	28.75	29.70 (29.04)	35.60 (30.34)	50.99 (34.40)	**28.41**	**29.59 (28.85)**	**34.15 (29.98)**	**45.18 (33.10)**
0.75	21.71	22.24 (21.83)	24.62 (22.40)	30.61 (24.11)	**13.61**	**14.08 (13.71)**	**16.64 (14.36)**	**23.52 (16.13)**	14.90	15.27 (15.00)	17.89 (15.60)	24.11 (17.28)

1.00	15.77	16.12 (15.86)	17.85 (16.33)	21.93 (17.45)	**8.21**	**8.53 (8.26)**	**9.92 (8.70)**	**13.76 (9.67)**	9.34	9.65 (9.39)	11.21 (9.81)	15.11 (10.83)
1.25	12.43	12.69 (12.5)	14.00 (12.83)	17.09 (13.71)	**5.61**	**5.85 (5.66)**	**6.78 (5.94)**	**9.36 (6.58)**	6.54	6.76 (6.60)	7.77 (6.87)	10.54 (7.57)
1.50	10.28	10.48 (10.31)	11.53 (10.59)	14.05 (11.33)	**4.17**	**4.32 (4.22)**	**4.99 (4.38)**	**6.82 (4.84)**	5.00	5.09 (5.01)	5.87 (5.19)	7.82 (5.69)
1.75	8.75	8.94 (8.81)	9.83 (9.03)	11.90 (9.63)	**3.26**	**3.37 (3.30)**	**3.88 (3.43)**	**5.29 (3.77)**	4.00	4.10 (4.00)	4.67 (4.14)	6.15 (4.54)
2.00	7.64	7.80 (7.69)	8.57 (7.89)	10.37 (8.41)	**2.67**	**2.74 (2.68)**	**3.16 (2.78)**	**4.21 (3.07)**	3.33	3.41 (3.34)	3.87 (3.46)	5.05 (3.77)
2.25	6.79	6.93 (6.84)	7.61 (7.00)	9.16 (7.45)	**2.23**	**2.29 (2.22)**	**2.63 (2.33)**	**3.50 (2.56)**	2.83	2.90 (2.85)	3.29 (2.96)	4.25 (3.20)
2.50	6.13	6.24 (6.16)	6.84 (6.31)	8.24 (6.72)	**1.92**	**1.98 (1.93)**	**2.26 (2.00)**	**2.97 (2.19)**	2.45	2.53 (2.47)	2.86 (2.56)	3.66 (2.78)
2.75	5.59	5.69 (5.62)	6.22 (5.75)	7.49 (6.10)	**1.69**	**1.74 (1.70)**	**1.97 (1.76)**	**2.58 (1.91)**	2.14	2.20 (2.15)	2.50 (2.22)	3.23 (2.44)
3.00	5.14	5.23 (5.16)	5.72 (5.29)	6.86 (5.61)	**1.51**	**1.55 (1.52)**	**1.74 (157)**	**2.26 (1.70)**	1.88	1.93 (1.89)	2.22 (1.96)	2.87 (2.15)
$\boldsymbol{EARL_1}$	39.04	39.86 (39.2)	44.80 (40.49)	56.53 (43.69)	38.32	39.70 (39.04)	46.58 (40.75)	63.26 (45.01)	**33.46**	**34.54 (33.95)**	**39.58 (35.24)**	**51.89 (38.56)**
$\boldsymbol{EARL_2}$	9.78	9.98 (9.83)	10.98 (10.09)	13.35 (10.77)	**3.93**	**4.07 (3.97)**	**4.70 (4.13)**	**6.42 (4.57)**	4.72	4.84 (4.74)	5.55 (4.91)	7.39 (5.39)
$\boldsymbol{EARL_3}$	5.91	6.02 (5.95)	6.60 (6.09)	7.94 (6.47)	**1.84**	**1.89 (1.84)**	**2.15 (1.92)**	**2.83 (2.09)**	2.33	2.39 (2.34)	2.72 (2.42)	3.50 (2.64)
$\boldsymbol{EARL_4}$	24.41	24.92 (24.51)	27.89 (25.29)	34.94 (27.23)	21.12	21.89 (21.50)	25.64 (22.44)	34.84 (24.79)	**19.09**	**19.69 (19.35)**	**22.56 (20.07)**	**29.64 (21.98)**
$\boldsymbol{EARL_5}$	7.84	8.00 (7.89)	8.79 (8.09)	10.65 (8.62)	**2.88**	**2.98 (2.90)**	**3.43 (3.02)**	**4.62 (3.33)**	3.52	3.62 (3.54)	4.13 (3.67)	5.45 (4.02)
$\boldsymbol{EARL_6}$	18.24	18.62 (18.32)	20.79 (18.89)	25.94 (20.31)	14.69	15.22 (14.94)	17.81 (15.60)	24.17 (17.22)	**13.5**	**13.92 (13.68)**	**15.95 (14.19)**	**20.93 (15.53)**

Illustrative examples

Example 1: Yogurt cup filling process

In order to illustrate the implementation of the HWMA $\bar{X}^*$ scheme with measurement errors, the data from Costa and Castagliola (2011) shown in Table 6 is used, assuming that A=0 and B=1 and that the data is subjected to a constant variance in the measurement system. The data is based on a yogurt cup filling process where the quality characteristic $X^*_{i,j,k}$ is the weight of each yogurt cup. In this example, it is assumed that the IC mean and the IC standard deviation are given by $\mu_0 = 124.90g$ and $\sigma_0 = 0.76g$, respectively. An independent R&R study estimated the measurement standard deviation $\sigma_m = 0.24$, yielding $\gamma = 0.24/0.76 = 0.316$. The quality practitioner in charge of this process decided to take, every hour, two sets of measurements, each of size $n = 5$ (i.e. $r = 2$ and $n = 5$). For a nominal ARL_0 value of 500

and $\lambda = 0.1$, it is found that $L^* = 2.938$ that yields an attained ARL_0 of 499.49. Thus, when r = 2, the lower and upper control limits of the HWMA $\bar{X}^*$ scheme when $i = 1$ and 2 are calculated using Equation (8) as follows:

$$LCL_i = \begin{cases} 124.90 - 2.938\sqrt{\frac{0.1^2}{5}\left(\frac{2+(0.316)^2}{2}\right)} = 124.80, & i = 1 \quad (17a) \\ 124.90 - 2.938\sqrt{\left(\frac{0.1^2}{5} + \frac{(1-0.1)^2 \times (0.76)^2}{5 \times (2-1)}\right)\left(\frac{2+(0.316)^2}{2}\right)} = 123.97, & i = 2 \quad (17b) \end{cases}$$

and

$$UCL_i = \begin{cases} 124.90 + 2.938\sqrt{\frac{0.1^2}{5}\left(\frac{2+(0.316)^2}{2}\right)} = 125.00, & i = 1 \quad (18a) \\ 124.90 + 2.938\sqrt{\left(\frac{0.1^2}{5} + \frac{(1-0.1)^2 \times (0.76)^2}{5 \times (2-1)}\right)\left(\frac{2+(0.316)^2}{2}\right)} = 125.83, & i = 2 \quad (18b) \end{cases}$$

For $i > 2$, the rest of the time-varying control limits can also be calculated in a similar way as shown in Equations (17b) and (18b), respectively. For illustration purpose, the first three plotting statistics are calculated as follows:

$\bar{X}_1^* = \frac{124.9+125.9+\cdots+124.1+124.4}{10} = 124.94$ and $\bar{\bar{X}}_0^* = \mu_0 = 124.90$,

$\bar{X}_2^* = \frac{124.9+125.5+\cdots+125.2+125.6}{10} = 124.96$ and $\bar{\bar{X}}_1^* = \frac{\bar{X}_1^*}{1} = 124.94$,

$\bar{X}_3^* = \frac{125.1+125.2+\cdots+122.4+125.4}{10} = 124.70$ and $\bar{\bar{X}}_2^* = \frac{\bar{X}_1^*+\bar{X}_2^*}{2} = \frac{124.94+124.96}{2} = 124.95$,

so that,

$H_1^* = \lambda\bar{X}_1^* + (1-\lambda)\,\bar{\bar{X}}_0^* = 0.1(124.94) + (1-0.1)124.90 = 124.904$,

$H_2^* = \lambda\bar{X}_2^* + (1-\lambda)\,\bar{\bar{X}}_1^* = 0.1(124.96) + (1-0.1)124.94 = 124.942$,

$H_3^* = \lambda\bar{X}_3^* + (1-\lambda)\,\bar{\bar{X}}_2^* = 0.1(124.70) + (1-0.1)124.95 = 124.925$.

The rest of the plotting statistics of the HWMA $\bar{X}^*$ scheme with 2-measurements are empirically shown in Table 6 and graphically in Figure 8. It is observed that the HWMA $\bar{X}^*$ scheme give an OOC signal for the first time on the 13th subgroup.

Table 6: Illustration of the implementation of the HWMA $\bar{X}^*$ scheme using the yogurt cup filling data

i	$X^*_{i,1,1}$	$X^*_{i,1,2}$	$X^*_{i,2,1}$	$X^*_{i,2,2}$	$X^*_{i,3,1}$	$X^*_{i,3,2}$	$X^*_{i,4,1}$	$X^*_{i,4,2}$	$X^*_{i,5,1}$	$X^*_{i,5,2}$	$\bar{X}^*_i$	$\bar{\bar{X}}^*_{i-1}$	H^*_i	LCL_i	UCL_i	Signal
1	124.9	124.8	125.9	125.9	125.2	124.8	124.6	124.1	124.8	124.4	124.94	124.90	124.90	124.80	125.00	No
2	124.9	125.2	125.5	125.0	124.1	123.9	125.2	125.2	125.0	125.6	124.96	124.94	124.94	123.97	125.83	No
3	125.1	125.1	125.2	124.8	125.4	125.3	122.9	122.4	125.4	125.4	124.70	124.95	124.93	124.24	125.56	No
4	126.1	125.9	124.6	124.8	125.7	125.5	126.4	126.5	124.9	125.7	125.61	124.87	124.94	124.36	125.44	No
5	125.8	125.7	122.6	122.6	124.1	123.5	126.1	126.3	124.9	125.0	124.66	125.05	125.01	124.43	125.37	No
6	125.0	125.2	125.5	124.8	124.8	125.0	124.9	124.8	124.8	124.2	124.90	124.97	124.97	124.48	125.32	No
7	124.2	124.6	125.8	125.3	125.4	125.5	126.4	126.2	125.1	125.2	125.37	124.96	125.00	124.51	125.29	No
8	124.9	124.9	123.8	123.2	125.1	125.3	124.0	124.5	124.4	124.2	124.43	125.02	124.96	124.54	125.26	No
9	125.9	125.8	124.4	124.8	126.3	125.7	124.9	125.2	125.2	125.1	125.33	124.95	124.98	124.56	125.24	No
10	124.2	124.3	126.2	125.5	125.6	125.0	124.4	124.4	124.1	124.3	124.80	124.99	124.97	124.58	125.22	No
11	123.7	123.6	123.4	123.3	124.7	124.8	123.1	123.1	123.1	122.8	123.56	124.97	124.83	124.59	125.21	No
12	124.0	124.1	122.6	122.4	123.6	123.6	124.4	124.5	123.6	123.1	123.59	124.84	124.72	124.60	125.20	No
13	122.0	122.5	123.9	124.0	123.7	124.1	124.3	124.4	121.9	122.9	123.37	124.74	124.60	124.62	125.18	Yes
14	122.4	123.0	122.8	123.1	123.7	124.2	123.7	124.1	122.8	123.1	123.29	124.63	124.50	124.62	125.18	Yes
15	123.9	123.6	124.1	124.5	123.4	122.9	123.1	123.1	124.5	125.1	123.82	124.54	124.46	124.63	125.17	Yes
16	121.9	122.3	123.4	123.3	123.5	123.3	125.3	125.5	123.3	123.6	123.54	124.49	124.39	124.64	125.16	Yes
17	123.3	122.9	123.6	123.5	124.2	123.8	123.4	123.6	123.5	123.4	123.52	124.43	124.34	124.65	125.15	Yes
18	122.0	122.2	123.6	123.4	124.7	125.0	122.6	122.5	124.5	123.9	123.44	124.38	124.28	124.65	125.15	Yes
19	124.0	123.9	123.1	123.4	123.9	124.5	122.6	122.8	124.2	123.5	123.59	124.32	124.25	124.66	125.14	Yes
20	125.5	124.9	122.2	122.3	123.2	123.2	123.2	123.3	123.2	123.2	123.42	124.29	124.20	124.67	125.13	Yes

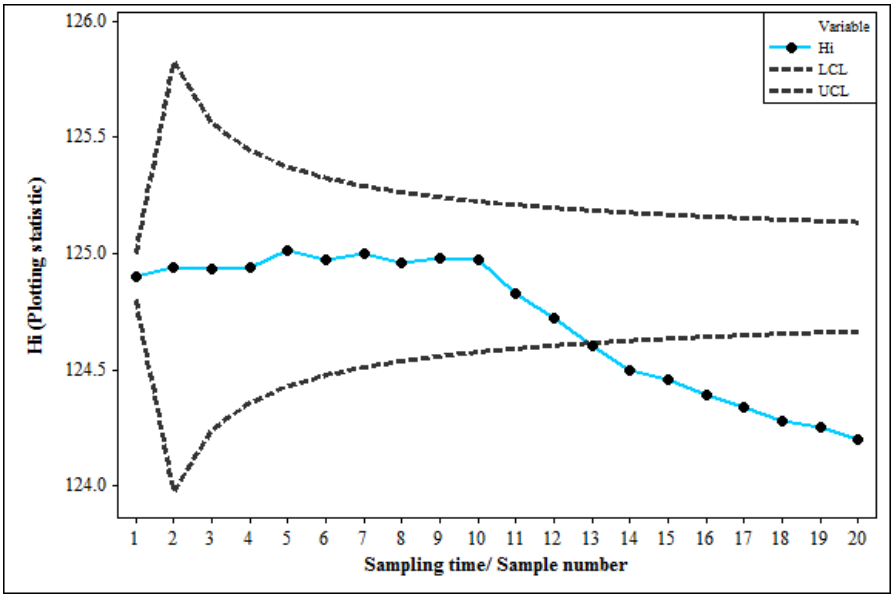

Figure 8: Illustrative example of the HWMA $\bar{X}^*$ scheme using the yogurt cup filling data

Example 2: Piston rings measurements

To illustrate the negative effect of increasing measurement errors from γ=0 to γ=0.9 without the use of multiple measurements, consider the dataset from Montgomery (2013) on the inside diameters in millimeter (*mm*) of piston rings manufactured by a forging process. This dataset contains 15 samples each of n = 5 observations. From the historical data, it is shown in Chapter 6 of Montgomery (2013) that the IC mean and the IC standard deviation are given by $\mu_0 = 74.0011mm$ and σ_0 = $0.0094mm$, respectively. Assuming that A=0, B=1, and a nominal ARL_0 value of 500, taking $\lambda = 0.1$ and $L^* = 2.938$ then the corresponding plotting statistics of the HWMA $\bar{X}^*$ scheme are given in Table 7. For γ=0 and 0.9, the corresponding time-varying control limits are as shown in Table 7 and Figure 9. It is observed that, for the same dataset, when γ=0 and 0.9, the HWMA $\bar{X}^*$ scheme gives the first OOC signal at the sample number 12 and 13, respectively. That is, HWMA $\bar{X}^*$ scheme in Figure 9 shows that the control limits for γ=0.9 are wider than those of γ=0. Thus, when the measurement error is relatively large, there is a delay in the signaling event of the HWMA $\bar{X}^*$ scheme when compared to a process with no measurement errors.

Table 7: Illustration of the implementation of the HWMA $\bar{X}^*$ scheme using the piston rings data

									γ=0.0		γ=0.9	
i	$X^*_{i,1,1}$	$X^*_{i,2,1}$	$X^*_{i,3,1}$	$X^*_{i,4,1}$	$X^*_{i,5,1}$	$\bar{X}^*_i$	$\bar{\bar{X}}^*_{i-1}$	H^*_i	LCL_i	UCL_i	LCL_i	UCL_i
1	74.012	74.015	74.030	73.986	74.000	74.009	74.001	74.002	74.000	74.002	74.000	74.003
2	73.995	74.010	73.990	74.015	74.001	74.002	74.009	74.008	73.990	74.012	73.988	74.015
3	73.987	73.999	73.985	74.000	73.990	73.992	74.005	74.004	73.993	74.009	73.991	74.011
4	74.008	74.010	74.003	73.991	74.006	74.004	74.001	74.001	73.995	74.008	73.993	74.009
5	74.003	74.000	74.001	73.986	73.997	73.997	74.002	74.001	73.996	74.007	73.994	74.008
6	73.994	74.003	74.015	74.020	74.004	74.007	74.001	74.001	73.996	74.006	73.995	74.007
7	74.008	74.002	74.018	73.995	74.005	74.006	74.002	74.002	73.996	74.006	73.995	74.007
8	74.001	74.004	73.990	73.996	73.998	73.998	74.002	74.002	73.997	74.006	73.996	74.007
9	74.015	74.000	74.016	74.025	74.000	74.011	74.002	74.003	73.997	74.005	73.996	74.006
10	74.030	74.005	74.000	74.016	74.012	74.013	74.003	74.004	73.997	74.005	73.996	74.006
11	74.001	73.990	73.995	74.010	74.024	74.004	74.004	74.004	73.997	74.005	73.997	74.006
12	74.015	74.020	74.024	74.005	74.019	74.017	74.004	74.005	73.998	74.005	73.997	74.006
13	74.035	74.010	74.012	74.015	74.026	74.020	74.005	74.006	73.998	74.005	73.997	74.005
14	74.017	74.013	74.036	74.025	74.026	74.023	74.006	74.008	73.998	74.005	73.997	74.005
15	74.010	74.005	74.029	74.000	74.020	74.013	74.007	74.008	73.998	74.004	73.997	74.005

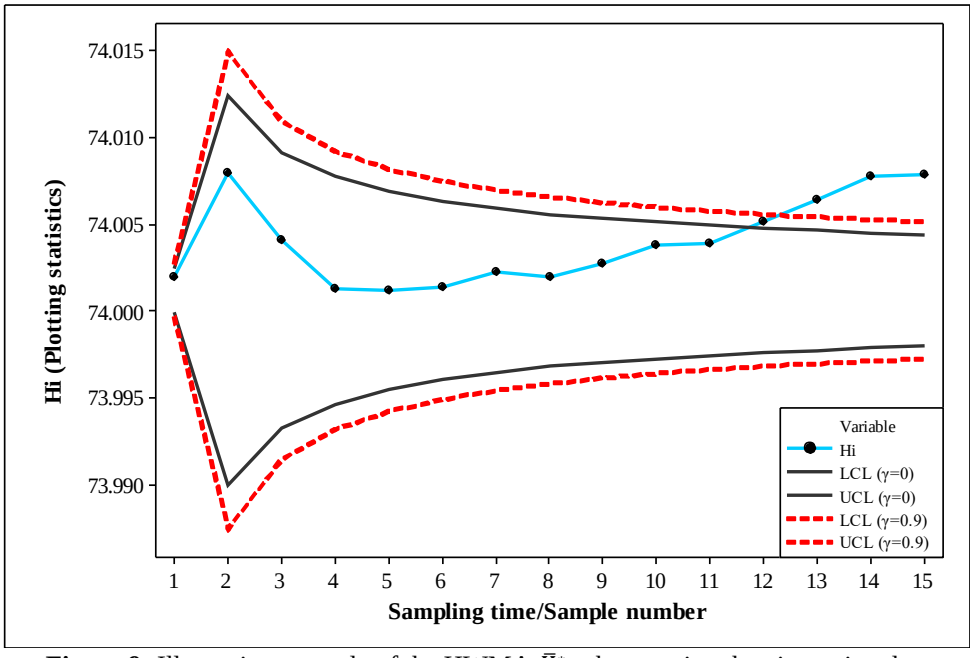

Figure 9: Illustrative example of the HWMA $\bar{X}^*$ scheme using the piston ring data

Conclusion

Most of the SPM schemes are based on the assumption of known process parameters under perfect measurements. This paper contributes to the SPM literature with an extensive investigation of the performance (or sensitivity) of the HWMA $\bar{X}^*$ scheme to monitor the process mean under the assumption of imperfect measurements using a constant and linearly increasing variance error model in the measurement system. A remedial approach that involves multiple measurements is implemented in the HWMA $\bar{X}^*$ scheme and it shows that it has a positive outcome in reducing the negative effect of measurement errors. Since multiple measurements increase cost and time in process monitoring, the negative effect of measurement errors can also be reduced by increasing the value of B in the covariate error model. Based on the sensitivity analysis, practitioners are not advised to use more than four measurements in the design of the HWMA $\bar{X}^*$ scheme regardless of the level of measurement error. Compared to the CUSUM scheme, the HWMA scheme is found to be superior regardless of the size of the mean shift. However, the HWMA scheme is superior to the EWMA scheme under small shifts only. In terms of the overall performance measure, the HWMA scheme outperforms the EWMA scheme for small, small-to-moderate and small-to-large shifts in the process mean. However, the latter performs better than the HWMA scheme under moderate, large and moderate-to-large shifts in the process mean.

Note that the HWMA $\bar{X}^*$ scheme is designed under the assumption of normally distributed data; however, when this assumption is violated, the properties of the HWMA $\bar{X}^*$ scheme need to be reinvestigated. Moreover, researchers can also investigate the sensitivity of the HWMA scheme to monitor autocorrelated observations with and without measurement errors.

Appendix: Simulation Algorithm

The computation of the IC and OOC run-length (*RL*) properties for the HWMA $\bar{X}$ scheme in the case of a standard normal distribution using w simulation runs are described below. The computation is done in

two stages; i.e. on the first stage, a search for the design parameter(s) that gives an attained IC *ARL* as close as possible to the nominal ARL_0 is conducted and if such design parameters exist, they are called the optimal design parameters; and on the second stage, these optimal design parameters are used to compute OOC *ARL* values.

First stage - Search of the optimal design parameter L^*:

Step 1. Specify the nominal ARL_0, A, B, C, D, γ, r, n, w, λ and the IC process parameters μ_0 and σ_0.

Step 2. (a) Fix a first value of L^* and calculate the control limits and go to Step 3.

(b) If required, increase (or decrease) L^* and recalculate the control limits so that the attained IC *ARL* get closer to the nominal ARL_0.

Step 3. Randomly generate a sample from the $N(A + B\mu_0, B^2\sigma_0^2 + C + D\mu_0)$ distribution. Calculate the charting statistic and compare it to the control limits found in Step 2. If the charting statistic plots between the control limits, then collect the next subgroup and calculate its charting statistic and compare it to the control limits. Continue this process until a sample point plots beyond the control limits. Then, record the number of samples plotted until an OOC signal occurs, this represents one value of the IC *RL* (RL_0) distribution. Repeat Step 3 a total of w times to find the $(w \times 1)$ RL_0 vector.

Step 4. Once the RL_0 vector is obtained, calculate the attained IC *ARL* $(= \frac{1}{w}\sum_{i=1}^{w} RL_{0_i})$. If the attained IC *ARL* is equal or much closer to the nominal ARL_0, go to Step 5. Otherwise, go back to Step 2(b) (i.e., since the attained IC ARL is considerably greater (smaller) than the nominal value, then update the control limit(s) narrower (wider) and repeat again Steps 3 and 4).

Step 5. The design parameter L^* found in Step 4 is called the optimal design parameter. Record the optimal L^* and its corresponding control limits. Thus, the search of the optimal L^* is completed.

Second stage - Computation of the characteristics of the OOC RL (RL_1):

Step 6. For a specific shift δ ($\delta \neq 0$) and γ, randomly generate a test sample from the $N(A + B(\mu_0 + \delta\sigma_0), B^2\sigma_0^2 + C + D\mu_0)$ distribution. Calculate the charting statistic(s) and compare to the control limit(s) found in Step 5. If the charting statistic plots between the control limits, then collect the next sample and calculate its charting statistic and compare it to the control limits. Continue this process until a sample point plots beyond the control limits. Then, record the number of subgroups plotted until an OOC signal occurs. This number represents one value of the RL_1 distribution. Repeat Step 6 a total of w times to find the $(w \times 1)$ RL_1 vector.

Step 7. Once the RL_1 vector is obtained, calculate the OOC *ARL* value $(= \frac{1}{w}\sum_{i=1}^{w} RL_{1_i})$.

Step 8. The computation of the characteristics of the RL_1 is completed.

Note that in Steps 4 and 7, other characteristics of the *RL* such as the standard deviation of the run-length (*SDRL*) can also be computed. More importantly, throughout this paper, w=50000 simulation runs are used in an effort to obtain accurate *RL* values.

Declaration of conflicting interests

The authors declared no potential conflict of interests with respect to the research, authorship and/or publication of this article.

Acknowledgements

The authors would like to thank the three anonymous reviewers; the Executive and Associate editors for taking their valuable time to evaluate our manuscript and gave constructive comments to improve it.

References

Abbas N, Riaz M and Does RJJJ (2013) Mixed exponentially weighted moving average-cumulative sum charts for process monitoring. *Quality and Reliability Engineering International* 29(3):345-356.

Abbas N (2018) Homogeneously weighted moving average control chart with an application in substrate manufacturing process. *Computers & Industrial Engineering* 120: 460-470.

Abbas N, Riaz M, Ahmad S, Abid M and Zaman B (2020) On the efficient monitoring of multivariate processes with unknown parameters. *Mathematics* 8(5):823. doi: 10.3390/math8050823.

Abbasi SA (2016) Exponentially weighted moving average chart and two-component measurement error. *Quality and Reliability Engineering International* 32(2):499-504.

Abid M, Shabbir A, Nazir HZ, Sherwani RAK and Riaz M (2020) A double homogeneously weighted moving average control chart for monitoring of the process mean. *Quality and Reliability Engineering International*, DOI: 10.1002/qre.2641.

Adegoke NA, Smith ANH, Anderson MJ, Sanusi RA and Pawley MDM (2019a) Efficient homogeneously weighted moving average chart for monitoring process mean using an auxiliary variable. *IEEE Access* 7:94021-94032.

Adegoke NA, Abbasi SA, Smith ANH, Anderson MJ and Pawley MDM (2019b) A multivariate homogeneously weighted moving average control chart. *IEEE Access* 7:9586-9597.

Adeoti OA (2020) On control chart for monitoring exponentially distributed quality characteristic. *Transactions of the Institute of Measurement and Control* 42(2):295-305.

Adeoti OA and Koleoso SO (2020) A hybrid homogeneously weighted moving average control chart for process monitoring. *Quality and Reliability Engineering International*, doi: 10.1002/qre.2690.

Ali R and Haq A (2017) New memory-type dispersion control charts. *Quality and Reliability Engineering International* 33(8):2131-2149.

Asif F, Noor-ul-Amin M, and Khan S (2020) Hybrid exponentially weighted moving average control chart with measurement error. *Iranian Journal of Science and Technology, Transactions A: Science.* DOI: 10.1007/s40995-020-00879-3.

Aslam M and Ali MM (2019) *Testing and Inspection using acceptance sampling plans*. Singapore: Springer Nature Pte Ltd., DOI: 10.1007/978-981-13-9306-8.

Bakdi A, Kouadri A (2018) An improved plant-wide fault detection scheme based on PCA and adaptive threshold for reliable process monitoring: Application on the new revised model of Tennessee Eastman process. *Journal of Chemometrics* 32(5):e2978.

Bakdi A, Bounoua W, Mekhilef S, Halabi LM (2019) Nonparametric Kullback-divergence-PCA for intelligent mismatch detection and power quality monitoring in grid-connected rooftop PV. *Energy* 189:116366.

Bounoua W, Benkara AB, Kouadri A, Bakdi A (2020) Online monitoring scheme using principal component analysis through Kullback-Leibler divergence analysis technique for fault detection, *Transactions of the Institute of Measurement and Control* 42(6):1225-1238.

Capizzi G and Masarotto G (2010) Combined Shewhart–EWMA control charts with estimated parameters. *Journal of Statistical Computation and Simulation* 80(7):793-807.

Cheng X-B and Wang F-K (2018) VSSI median control chart with estimated parameters and measurement errors. *Quality and Reliability Engineering International* 34(5):867-881.

Haq A, Brown J and Moltchanova E (2013) New synthetic EWMA and synthetic CUSUM control charts for monitoring the process mean. *Quality and Reliability Engineering International* 32(1):269-290.

Linna KW and Woodall WH (2001) Effect of measurement error on Shewhart control charts. *Journal of Quality Technology* 33(2):213-222.

Maleki MR, Amiri A and Castagliola P (2017) Measurement errors in statistical process monitoring: A literature review. *Computers & Industrial Engineering* 103:316-329.

Malela-Majika J-C (2020) New distribution-free memory-type control charts based on the Wilcoxon rank-sum statistic. *Quality Technology & Quantitative Management*, DOI: 10.1080/16843703.2020.1753295.

Maravelakis P (2012) Measurement error on the CUSUM control chart. *Journal of Applied Statistics* 39(2):323-336.

Maravelakis P, Panaretos J and Psarakis S (2004) EWMA chart and measurement error. *Journal of Applied Statistics* 31(4):445-455.

Montgomery DC (2013) *Statistical Quality Control: A Modern Introduction*, 7th ed., Singapore: John Wiley & Sons.

Nguyen H-D, Nguyen TQ, Tran KP and Ho P (2019) On the performance of VSI Shewhart control chart for monitoring the coefficient of variation in the presence of measurement errors. *The International Journal of Advanced Manufacturing Technology* 104(1-4):211-243.

Noor-ul-Amin M, Javaid A, Hanif M and Dogu E (2020) Performance of maximum EWMA control chart in the presence of measurement error using auxiliary information. *Communications in Statistics - Simulation and Computation*, DOI: 10.1080/03610918.2020.1772301.

Page ES (1961) Cumulative sum charts. *Technometrics* 3(1):1-9.

Raza M, Nawaz T and Han D (2020) On designing distribution-free homogeneously weighted moving average control charts. *Journal Testing and Evaluation*, DOI: 10.1520/JTE20180550.

Riaz A, Noor-ul-Amin M, Shehzad MA and Ismail M (2019) Auxiliary information based mixed EWMA-CUSUM mean control chart with measurement error. Iranian Journal of Science and Technology, Transactions A: Science, 43(6):2937-2949.

Roberts SW (1959) Control charts tests based on geometric moving averages. *Technometrics* 1(3):239-250.

Sabahno H, Amiri A and Castagliola P (2019) Optimal performance of the variable sample sizes Hotelling's T^2 control chart in the presence of measurement errors. *Quality Technology & Quantitative Management* 16(5):588-612.

Sabahno H, Castagliola P and Amiri A (2020) A variable parameters multivariate control chart for simultaneous monitoring of the process mean and variability with measurement errors. *Quality and Reliability Engineering International* 36(4):1161-1196.

Salmasnia A, Maleki MR and Niaki STA (2018) Remedial measures to lessen the effect of imprecise measurement with linearly increasing variance on the performance of the Max-EWMAMS scheme. *Arabian Journal of Science and Engineering* 43(6):3151-3162.

Shongwe SC, Malela-Majika J-C, Castagliola P (2020a) A combined mixed-*s*-skip sampling strategy to reduce the effect of autocorrelation on the $\bar{X}$ scheme with and without measurement errors. *Journal of Applied Statistics*, DOI: 10.1080/02664763.2020.1759033.

Shongwe SC, Malela-Majika J-C, Castagliola P (2020b) The new synthetic and runs-rules schemes to monitor the process mean of autocorrelated observations with measurement errors. *Communications in Statistics - Theory and Methods*, DOI: 10.1080/03610926.2020.1737125.

Shongwe SC, Malela-Majika J-C, Castagliola P (2020c) On monitoring the process mean of autocorrelated observations with measurement errors using the w-of-w runs-rules scheme. *Quality and Reliability Engineering International* 36(3):1144-1160.

Tang AA, Castagliola P, Hu XL and Sun J (2019) The performance of the adaptive EWMA median chart in the presence of measurement error. *Quality and Reliability Engineering International* 35(1):423-438.

Tran KP, Heuchenne C, Balakrishnan N (2019a) On the performance of coefficient of variation charts in the presence of measurement errors. *Quality and Reliability Engineering International* 35(1):329-350.

Tran PH, Tran KP and Rakitzis AC (2019b) A synthetic median control chart for monitoring the process mean with measurement errors. *Quality and Reliability Engineering International* 35(4):1100-1116.

Tran KP, Nguyen HD, Tran PH and Heuchenne C (2019c) On the performance of CUSUM control charts for monitoring the coefficient of variation with measurement errors. *The International Journal of Advanced Manufacturing Technology* 104(5-8):1903-1917.

Tran KD, Nguyen HD, Nguyen TH and Tran KP (2020) Design of a variable sampling interval exponentially weighted moving average median control chart in presence of measurement errors. *Quality and Reliability Engineering International* DOI: 10.1002/qre.2726.

Umar AA, Khoo MBC, Saha Sand Haq A (2019) A combined variable sampling interval and double sampling control chart with auxiliary information for the process mean. *Transactions of the Institute of Measurement and Control*, DOI: 10.1177/0142331219885525.

Waldmann KH (1996) Design of double CUSUM quality control schemes. *European Journal Operational Research* 95(3):641-648.

Yeong WC, Khoo MBC, Lim SL and Teoh WL (2017) The coefficient of variation chart with measurement error. *Quality Technology & Quantitative Management* 14(4):353-377.

Zaidi FS, Castagliola P, Tran KP and Khoo MBC (2019) Performance of the Hotelling's T^2 control chart for compositional data in the presence of measurement errors. *Journal of Applied Statistics* 46(14):2583-2602.

Zaidi FS, Castagliola P, Tran KP and Khoo MBC (2020) Performance of the MEWMA-CoDa control chart in the presence of measurement errors. *Quality and Reliability Engineering International*, DOI: 10.1002/qre.2705.